

Electronic Supporting Information For

Trinitromethyl-Triazolone (TNMTO): A Highly Dense Oxidizer

Sohan Lal^a, Richard J. Staples^b, Jean'ne M. Shreeve^{a*}

^aDepartment of Chemistry, University of Idaho, Moscow,
Idaho 83844-2343

^bDepartment of Chemistry, Michigan State University, East
Lansing, Michigan 48824

To whom correspondence should be addressed. E-mail:

jshreeve@uidaho.edu. Fax: +1-208-885-9146

Entry	Table of Contents	Page
1	Table S1. Calculated Total Energy (E_0), Zero-point Energy (ZPE), values of Thermal Correction (HT) and Enthalpy of Formation ($\Delta_f H^\circ$ (g)) of the compounds	S3
2	Figure S1: Isodesmic reaction for TNMTO	S3
3	Table S2: The standard enthalpy of combustion ΔH_f° (combust) for TNMTO	S4
4	Figure S2. Computed electrostatic potential (ESP) maps of RDX, NTO, DNMTO	S4
5	Figure S3. Non-covalent interaction (NCI) plots for NTO and DNMTO	S5
6	Table S3. Comparison of the ratio of positive and negative ESPs	S5
7	Figure S4. Predicted UV-Visible spectrum of TNMTO	S6
8	Experimental section	S6-S9
9	Figure S5-S9. Single crystal X-ray structure of TNMTO	S10-S12
10	Tables S4-S10. Single crystal X-ray data of TNMTO	S12-S15
11	Table S11. Single crystal X-ray data of compound 9	S16
12	Table S12. Single crystal X-ray data of compound 11.H ₂ O	S17
13	Figures S10-S25. FTIR, ¹ H, ¹³ C NMR plots	S18-S25
14	Figures S26-S35. DSC plots of title compounds	S26-S30
15	Figures S36-S42. TGA plots of title compounds	S31-S34
16	Tables S13-S16. Cartesian coordinates (in Å) for the optimized structures	S34-S37
17	Figure S43. Comparison of bond dissociation energies	S37
18	Figure S44. Comparison of detonation velocity and detonation pressure	S38
19	Figure S45. Comparison of heat of detonation (Q).	S38
20	Figure S46. Comparison of characteristic velocity (C*)	S39
21	References	S39-S40

Table S1. Calculated Total Energy (E_0), Zero-point Energy (ZPE), values of Thermal Correction (H_T) and Enthalpy of Formation ($\Delta_f H^\circ$ (g)) of the title compounds using B3LYP/6-31+G**//MP2/6-311++G** level of theory (Isodesmic).

Compounds	E_0	ZPE	H_T	$\Delta_f H^\circ$ (g) kJ/mol	$\Delta_f H_{\text{sub}}^\circ$ kJ/mol	$\Delta_f H^\circ$ (s) kJ/mol
	[Hartree/Particle]	[Hartree/Particle]	[Hartree/Particle]			
CH ₄	-40.3796224	0.044793	0.003812	-74.60 ^a	----	----
CH ₃ NO ₂	-244.4784821	0.049840	0.005298	-74.30 ^a	----	----
CH ₃ CH ₃	-79.5716305	0.074610	0.004428	-84.00 ^a	----	----
TNE	-691.8636667	0.082007	0.011245	-91.63 ^a	----	----
TO	-316.7572189	0.064231	0.005616	-25.87 ^a	----	----
MTO	-355.9630511	0.091809	0.007306	-41.80 ^a	----	----
NTO, 5	-520.8511701	0.066465	0.007992	-20.55 ^a (-25.57) ^b	47.75 ^c	-68.30
TNMTO, 6	-968.2367424	0.097889	0.014696	-49.43 ^b	15.04 ^c	-64.47

[a] Obtained at G2 level. ^bCalculated using isodesmic equation as shown in Fig. S1. ^cCalculated using $\Delta H_{\text{sub}} = 0.188 \times T / \text{kJmol}^{-1} \text{K}^{-1}$

The gas-phase enthalpy of formation $\Delta_f H^\circ$ (g) was predicted using Gaussian 03 program¹ according to isodesmic equation as shown in Figure S1.

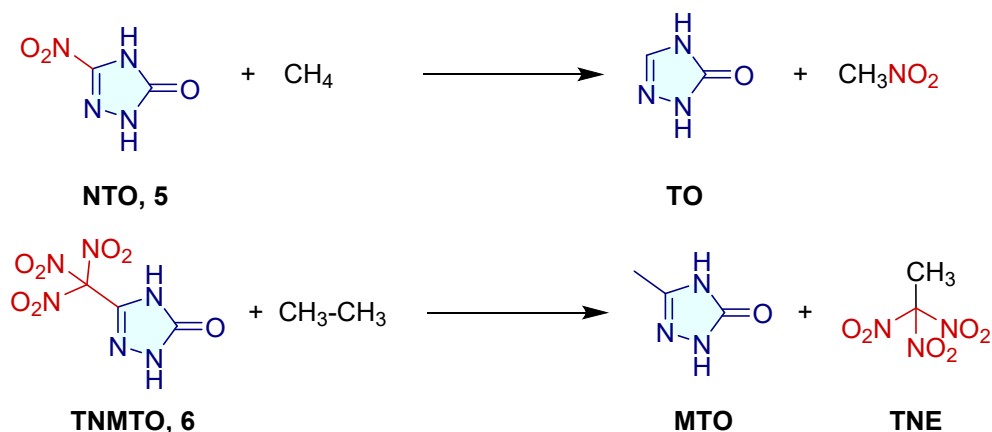


Fig. S1 Isodesmic reaction for TNMTO

Subsequently, for TNMTO, solid-phase enthalpy of formation $\Delta_f H^\circ$ (s) were calculated by using equation 1.²⁻⁴

$$\Delta_f H^\circ(\text{s}) = \Delta_f H^\circ(\text{g}) - \Delta H_{\text{sub}} \quad (1)$$

Where, $\Delta_f H^\circ$ (s) is solid phase enthalpy of formation, $\Delta_f H^\circ$ (g) is gas phase enthalpy of formation and ΔH_{sub} is the enthalpy of sublimation.

The enthalpy of sublimation was estimated using equation 2 as per Trouton's rule.⁵

$$\Delta H_{\text{sub}} = 0.188 \times T / \text{kJmol}^{-1} \text{K}^{-1} \quad (2)$$

where, T , is either the melting point (mp) or the decomposition temperature (T_d), when no melting happens before decomposition.

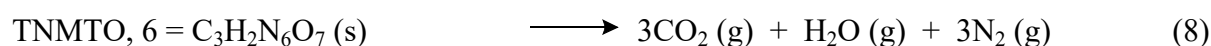
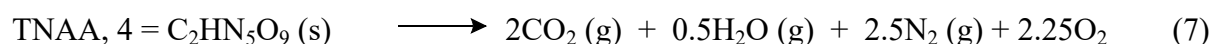
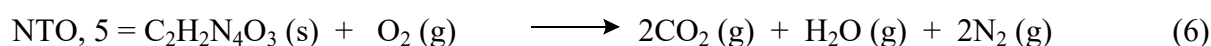
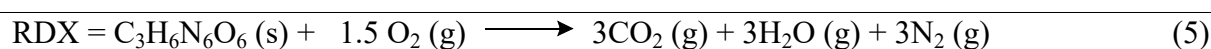
The bond dissociation energies (BDEs) of compounds TNMTO and TNAА were estimated according to following equation 3.

$$\text{BDE [AB]} = E_0 [\text{A.}] + E_0 [\text{B.}] - E_0 [\text{AB}] \quad (3)$$

where, BDE [AB] is bond dissociation energy and E_0 [A.] and E_0 [B.] are the energies of individual homolytic part and E_0 [AB] is the total energy of the individual molecule.

Table S2. The standard enthalpy of combustion ΔH_f° (combust) for the title compounds was calculated by following equation 8.

$$\Delta_f H^\circ_{(\text{combust})} = \sum \Delta_f H^\circ_{(\text{products})} - \sum \Delta_f H^\circ_{(\text{reactants})} \quad (4)$$



The standard enthalpy of formation for CO_2 ($\Delta H_f(\text{CO}_2) = -393.51 \text{ kJmol}^{-1}$); H_2O ($\Delta H_f(\text{H}_2\text{O}) = -243.015 \text{ kJmol}^{-1}$).

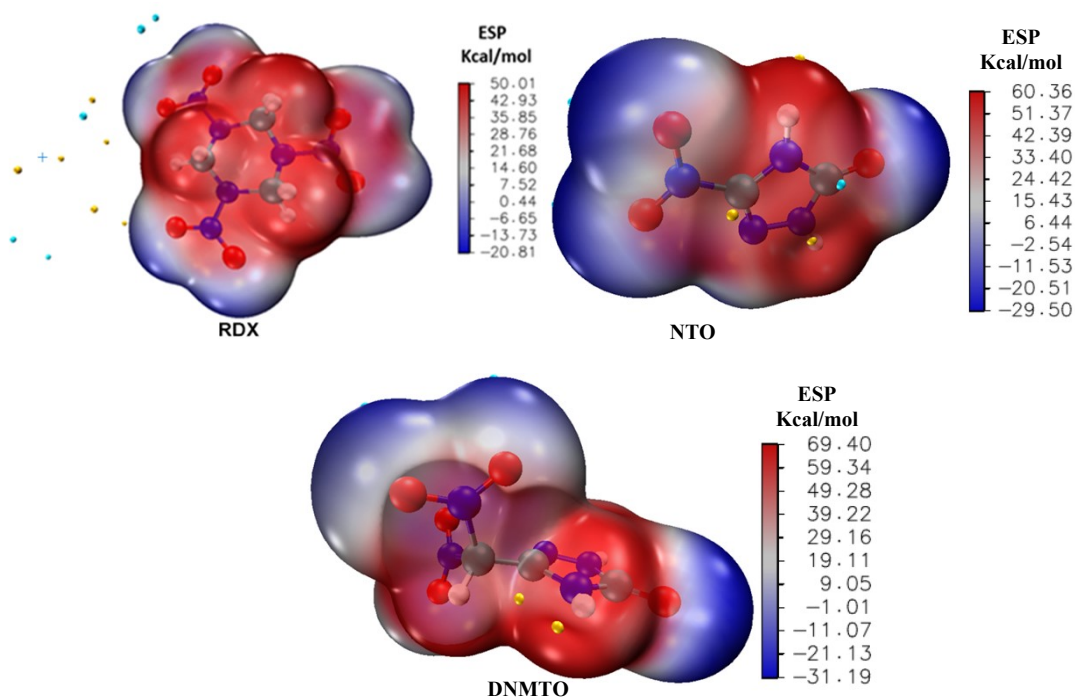


Fig. S2 Computed electrostatic potential (ESP) maps of RDX, NTO and DNMT0.

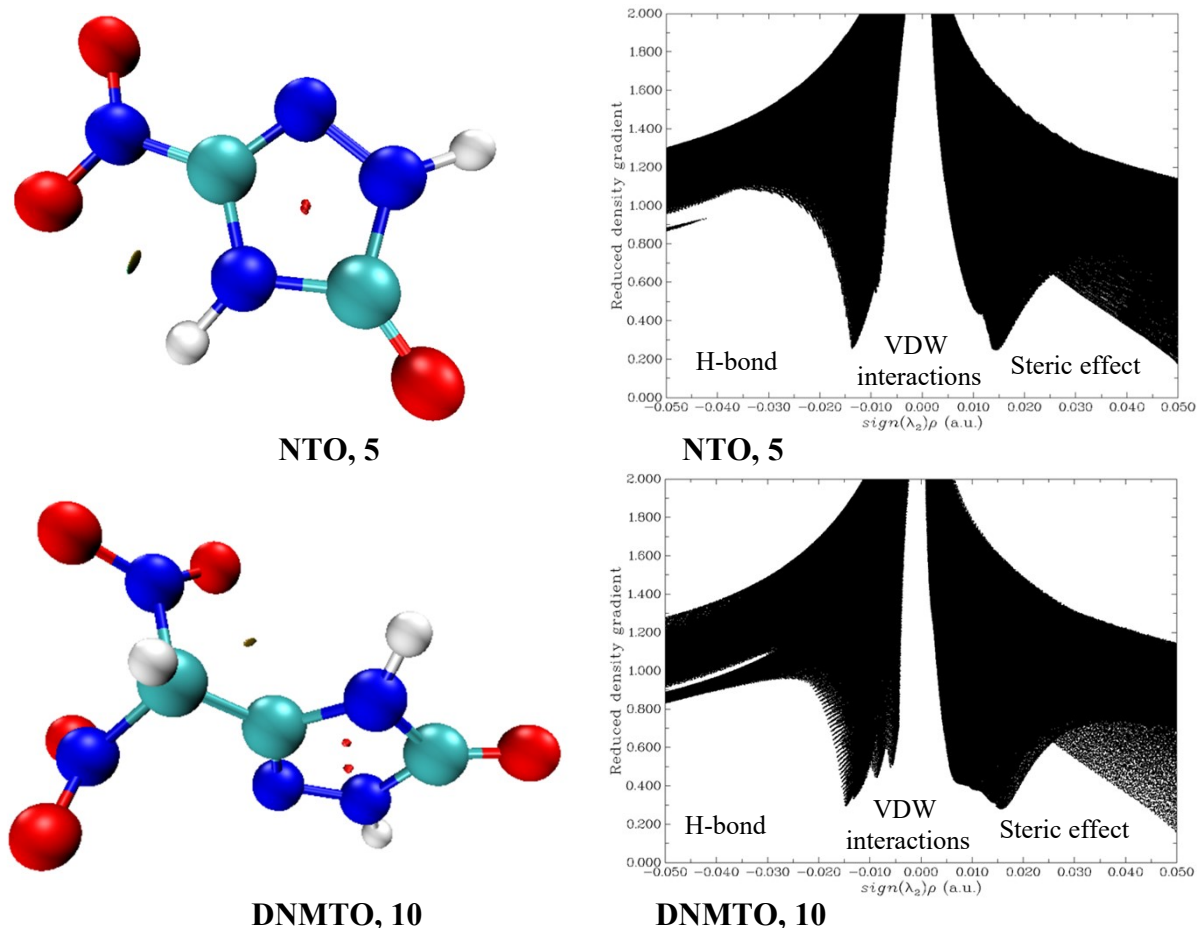


Fig. S3 Non-covalent interaction (NCI): Reduced density gradient (RDG) and scatter diagram of NTO and DNMT0.

Table S3. Comparison of the ratio of positive and negative ESPs and the surface area of ESPs of compounds and positive variance, total variance, balance of charges and product of total variance and balance of charges.

Compounds	A_{tot}^a \AA^2	A_{pos}^b \AA^2	A_{neg}^c \AA^2	ratio _{pos} (%)	ratio _{neg} (%)	$\sigma_{tot}^2 v^d$ (kcal/mol)
TNMTO, 6	205.40	102.51	102.89	49.90	50.10	38.80
DNMT0, 10	187.12	87.93	99.19	46.99	53.01	45.12
TNT	221.89	128.42	93.47	57.88	42.12	22.48
NTO, 5	139.77	73.55	66.22	52.62	47.38	43.76
RDX	209.49	116.77	92.72	55.74	44.26	27.29

^a SA_{tot} = Total surface area. ^b SA_{pos} = positive surface area. ^c SA_{neg} = Negative surface area. ^dRatio of positive surface area ^eRatio of negative surface area. ^gProduct of total variance and balance of charges.

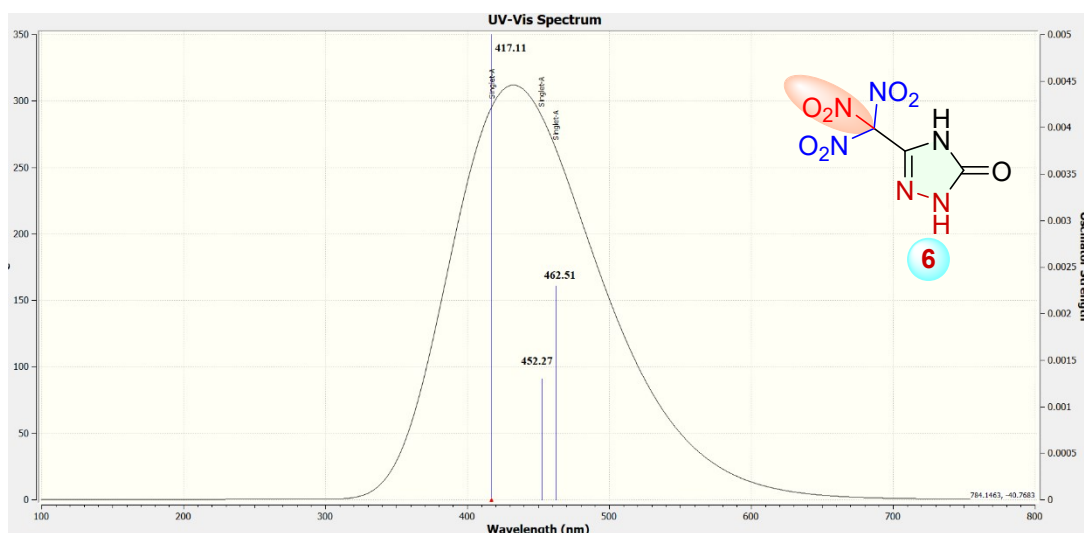


Fig. S4 Predicted UV-Visible spectrum of TNMTO at B3LYP/6-311++G(d,p) level.

EXPERIMENTAL SECTION

General Methods

All reagents and solvents were used as received unless otherwise specified (AKSci, Sigma-Aldrich, Acros Organics, VWR). The densities of the new compounds were measured at 25 °C with a Micromeritics Accupyc II 1340 gas pycnometer. Thermal stabilities (melting and decomposition points) were measured by heating individual samples from 35 to 400 °C at a heating rate of 5 °C min⁻¹ and 10 °C min⁻¹ on a Differential Scanning Calorimeter (DSC, TA Instruments Company, Model: Q2000) and thermogravimetric analysis (TGA, TA Instruments Company, Model: Q50). The FTIR spectra were recorded using KBr plates on a Thermo Nicolet AVATAR 370 spectrometer. ¹H and ¹³C NMR spectra were obtained on a 500 MHz (Bruker) nuclear magnetic resonance spectrometer operating at 500.19 and 125.77 MHz, respectively, using DMSO-d₆ as the solvent and locking solvent. The ¹⁵N NMR spectra were recorded on a 500.19 MHz (Bruker 500) nuclear magnetic resonance operating at 50.70 MHz. As external standards, the chemical shifts are given relative to tetramethylsilane (¹H, ¹³C) and nitromethane (¹⁵N). Elemental analyses (C, H, N) were performed on a Vario Micro cube Elemental Analyser.

The crystals of compounds 6, 9 and 11.H₂O were mounted on a nylon loop with Paratone oil on an XtaLAB Synergy, Dualflex, HyPix diffractometer at 100 K. The structures were solved with the ShelXT⁶⁻⁹ solution program using dual methods and Olex2.¹⁰ The model was refined with ShelXL⁶⁻⁹ using full matrix least squares minimization on F².

Caution!

The compounds studied are potentially high-energy materials. Therefore, it is strongly recommended that they should be synthesized in only small amounts and handled with extreme care.

5-(Trinitromethyl)-2,4-dihydro-3H-1,2,4-triazol-3-one (6). Compound 10 (1.89 g, 10.0 mmol, 1.0 equiv.) was added in portions to pre-cooled 100% HNO₃ (18.9 g, 12.6 mL, 300.0 mmol, 30.0 equiv.), at -10 °C. The reaction mixture was maintained at that temperature for another 5 h. The HNO₃ was evaporated to leave a slightly yellow solid which was triturated with DCM to give pure 6 in excellent yield. White solid, 2.15 g, 90% yield, DSC (5 °C min⁻¹): T_{d (onset)} = 80 °C. IR (KBr, ν, cm⁻¹) 3178 (s), 3053 (s), 2920 (s), 1715 (s), 1594 (s), 1476 (s), 1381 (s), 1278 (s), 1066 (s), 1031 (s), 944 (m), 803 (s), 777 (m), 735 (m); ¹H NMR (500.19 MHz, Acetone-d₆): δ 9.13 (br s, 1H), 12.35 (br s, 1H); ¹³C NMR (125.77 MHz, CD₃CN): δ 125.8, 132.8, 155.1; Elemental analysis: calcd (%) for C₃H₂N₆O₇ (234.08): C 15.39, H 0.86, 35.90; found: C 15.30, H 1.46, N 34.77. The compound reacted slowly with CD₃CN, and acetone-d₆, reacted vigorously with D₂O, and DMSO-d₆ and subsequently decomposed with an exothermic reaction. It is stable in anhydrous DCM and CHCl₃ at room temperature however, TNMTO is partially soluble in DCM and CHCl₃.

2-(Dinitromethylene)-5,5-dinitro-2,5-dihydropyrimidine-4,6-diol (8). 4,6-Dihydroxy-2-methylpyrimidine 7 (8.0 g, 63.49 mmol, 1.0 equiv.) was added in portions to conc. H₂SO₄ (64.0

g, 24.0 mL, 65.30 mmol, 1.03 equiv.) at 0 °C. The mixture was cooled to -10 °C, and 100% HNO₃ (54.0 g, 36.0 mL, 85.71 mmol, 1.58 equiv.) was added. After 1.5 h, the white precipitate was filtered off, immediately washed with TFA (20 mL) and trifluoroacetic anhydride (20 mL), and dried to give a white solid 8, Yield: 17.48 g, 90%, DSC (5 °C min⁻¹): T_{d (onset)} = 86 °C. IR (KBr, ν, cm⁻¹) 3600 (s), 3518 (s), 3326 (s), 3197 (s), 3061 (s), 1628 (s), 1528 (s), 1401 (s), 1343 (s), 1290 (s), 1207 (s), 1154 (s), 1132 (s), 1037 (s), 895 (m), 812 (m), 794 (m), 747 (s), 724 (s); ¹H NMR (500.19 MHz, CDCl₃): δ 7.66 (br s, 2H); ¹³C NMR (125.77 MHz, DMSO-d₆): δ 98.8, 107.1, 125.0, 158.2. Elemental analysis: calcd (%) for C₅H₂N₆O₁₀ (306.10): C 19.62, H 0.66, 27.46; found: C 19.70, H 1.09, N 27.64.

Hydrazinium 3-dinitromethanide-1,2,4-triazolone (9). Compound 8 (4.590 g, 15.0 mmol, 1.0 equiv.) was added portion-wise to hydrazine hydrate (20 mL, 40% solution in water) at 0 °C. The resulting yellow mixture was stirred for another 5 h. The excess hydrazine was quenched with conc. HCl at 0 °C, and the yellow precipitate was filtered off, washed with cold water, and dried to give pure 9 as a light-yellow solid. 2.85 g, 86%, DSC (5 °C min⁻¹): T_{d (onset)} = 178 °C. IR (KBr, ν, cm⁻¹) 3342 (s), 3289 (s), 3068 (m), 2988 (m), 2882 (m), 2635 (m), 1721 (s), 1629 (m), 1575 (m), 1545 (m), 1509 (s), 1454 (m), 1419 (w), 1341 (m), 1247 (s), 1141 (s), 1102 (s), 1080 (m), 1041 (m), 965 (m), 746 (m), 680 (m); ¹H NMR (500.19 MHz, DMSO-d₆): δ 7.1 (br s, 5H), 11.21 (br s, 1H), 11.48 s, 1H); ¹³C NMR (125.77 MHz, DMSO-d₆): δ 124.6, 139.6, 156.3; Elemental analysis: calcd (%) for C₃H₇N₇O₅ (221.13): C 16.29, H 3.19, 44.34; found: C 16.22, H 3.14, N 44.34.

5-(Dinitromethyl)-2,4-dihydro-3H-1,2,4-triazol-3-one (10). Compound 9 (4.42 g, 20.0 mmol, 1.0 equiv.) was dissolved in acetonitrile (100 mL), and HCl (12M, 3.0 mL) was added at 0 °C. The resulting mixture was then heated at 60 °C for 1 h. The white precipitate was removed by filtration, washed with acetonitrile and the filtrate was dried under air to give compound 10 in

pure form as a white solid, 3.0 g, 80%, DSC ($5\text{ }^{\circ}\text{C min}^{-1}$): $T_{d(\text{onset})} = 88\text{ }^{\circ}\text{C}$. IR (KBr, ν , cm^{-1}) 3175 (s), 3034 (s), 2954 (s), 1744 (s), 1697 (s), 1596 (s), 1515 (m), 1487 (m), 1383 (m), 1366 (m), 1325 (s), 1292 (m), 1235 (s), 1201 (s), 1127 (s), 1093 (s), 1039 (m), 1011 (m), 821 (m), 778 (m), 744 (m); $^1\text{H NMR}$ (500.19 MHz, acetone- d_6): δ 8.06 (s, 1H), 11.75 (s, 1H); $^{13}\text{C NMR}$ (125.77 MHz, acetone- d_6): δ 105.1, 134.9, 155.9; Elemental analysis: calcd (%) for $\text{C}_3\text{H}_3\text{N}_5\text{O}_5$ (189.09): C 19.06, H 1.60, 37.04; found: C 19.98, H 2.09, N 37.74.

Ammonium-6-(dinitromethylene)-11²,3,5-triazinane-2,4-dione ($11\cdot\text{H}_2\text{O}$). Compound 8 (4.590 g, 15.0 mmol, 1.0 equiv.) was added portion-wise to aqueous NH_3 (25 mL, 30% solution in water) at $0\text{ }^{\circ}\text{C}$. The resulting yellow mixture was stirred for 6 h. The yellow precipitate was filtered, washed with CH_3CN , and dried to give pure $11\cdot\text{H}_2\text{O}$ as a light-yellow solid (3.48 g, 92%), DSC ($5\text{ }^{\circ}\text{C min}^{-1}$): $T_{d(\text{onset})} = 200\text{ }^{\circ}\text{C}$. IR (KBr, ν , cm^{-1}); $^1\text{H NMR}$ (500.19 MHz, DMSO- d_6): δ 6.64 (br s, 4H); $^{13}\text{C NMR}$ (125.77 MHz, DMSO- d_6): δ 133.0, 157.5, 161.6; Elemental analysis: calcd (%) for $\text{C}_4\text{H}_8\text{N}_6\text{O}_7$ (252.14): C 19.05, H 3.20, 33.30; found: C 19.76, H 3.30, N 33.28.

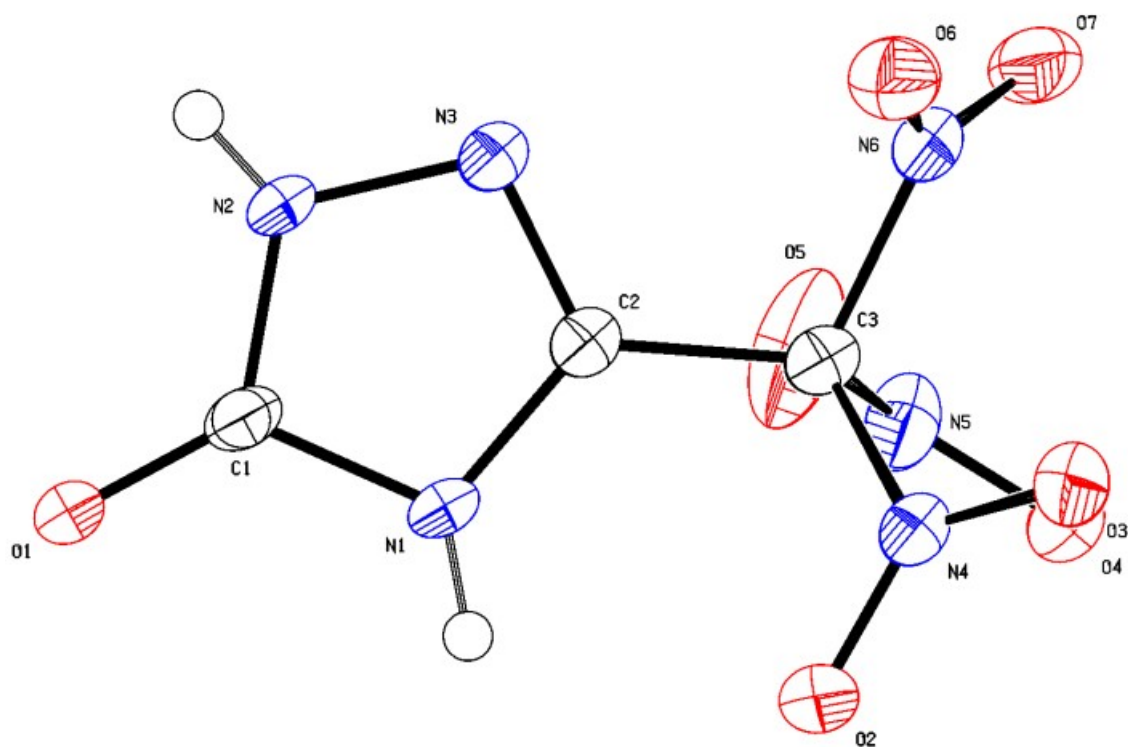


Fig. S5 Single crystal X-ray structure of TNMTO. Drawing at 50% ellipsoids with heteroatoms labelled and the hydrogen atoms found and refined isotropically.

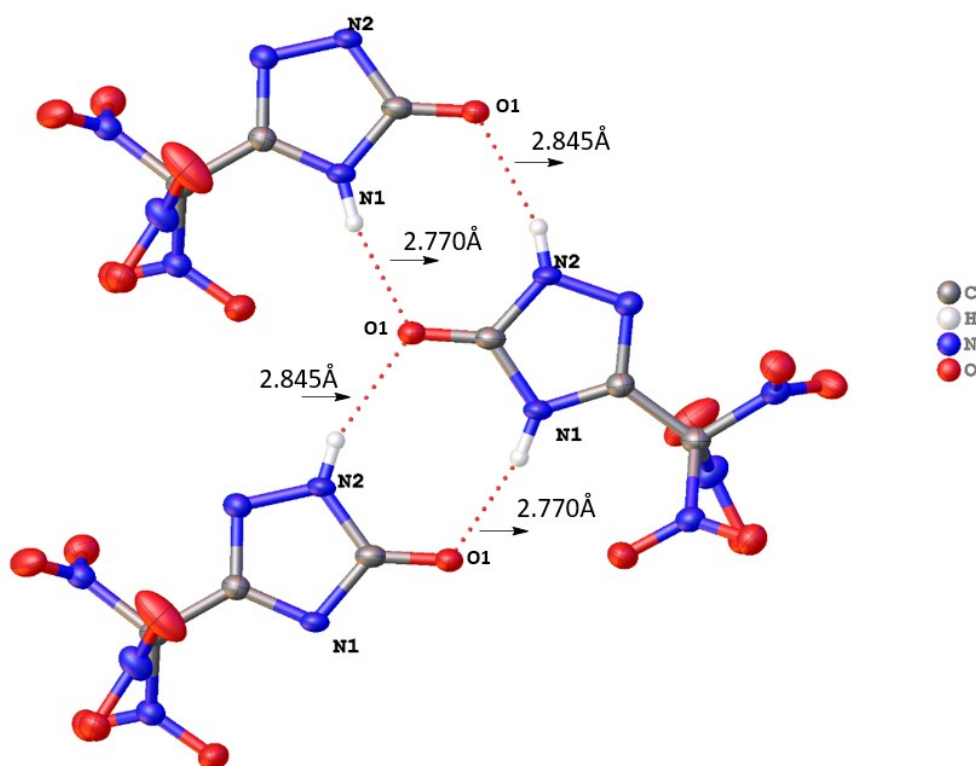


Fig. S6 The following hydrogen bonding interactions with a maximum D-D distance of 3.1 Å and a minimum angle of 110° are present in TNMTO: N1–O1₁: 2.77 Å, N2–O1₂: 2.845 Å.

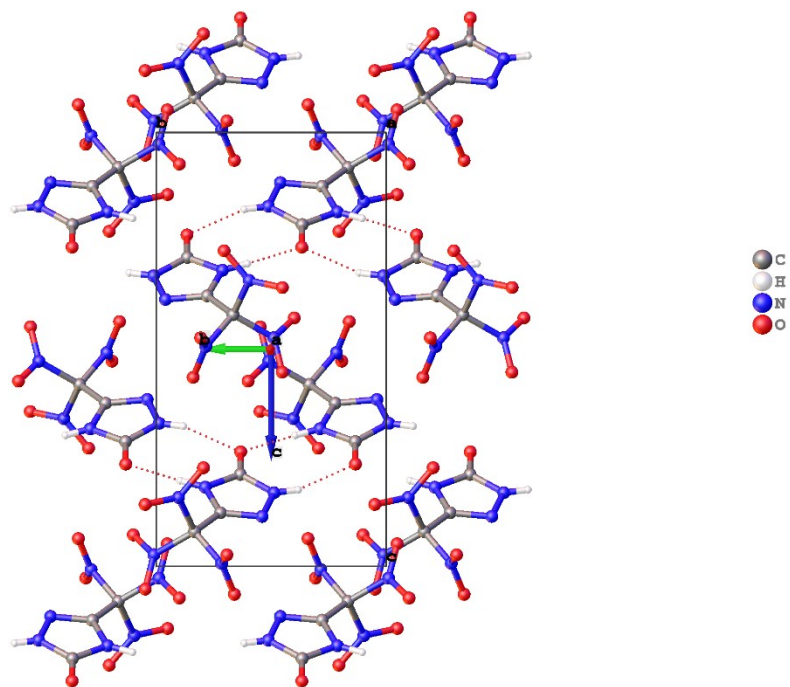


Fig. S7 Packing diagram of TNMTO viewed along a axis

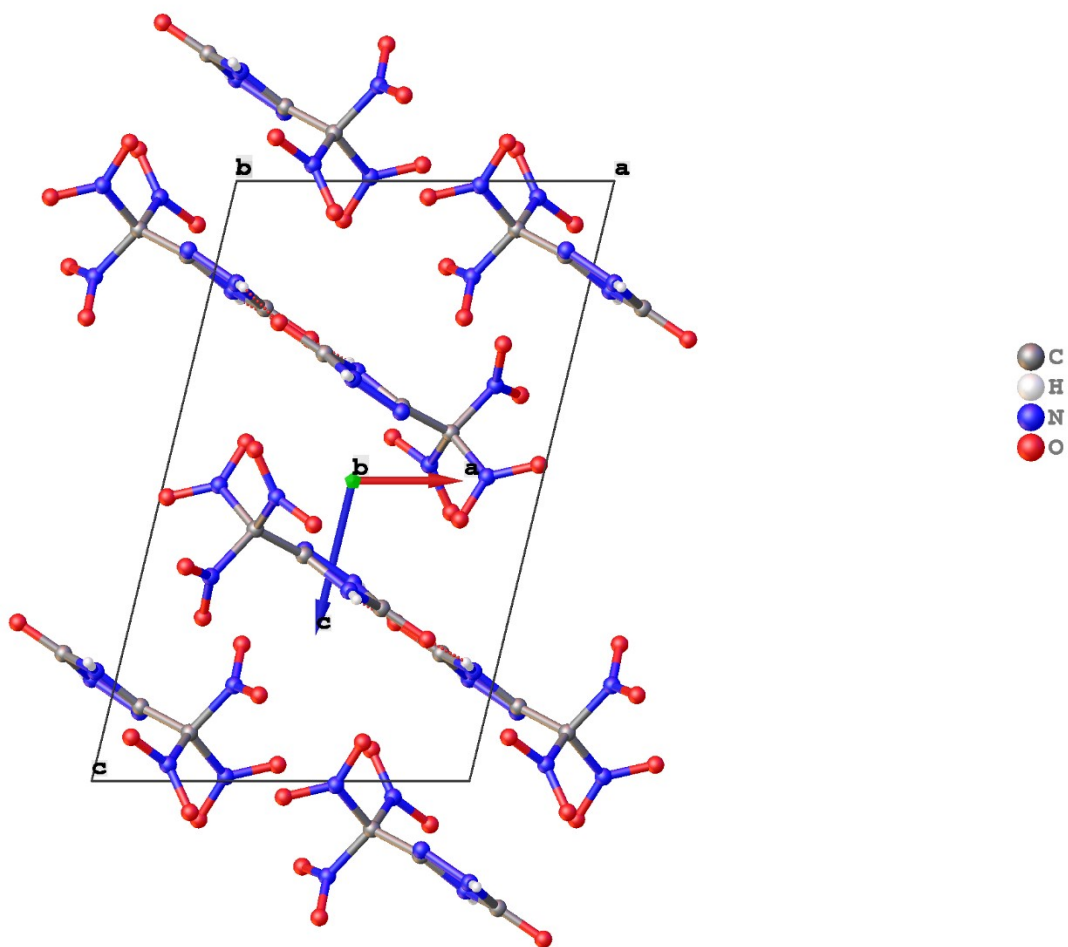


Fig. S8 Packing diagram of TNMTO viewed along the b axis

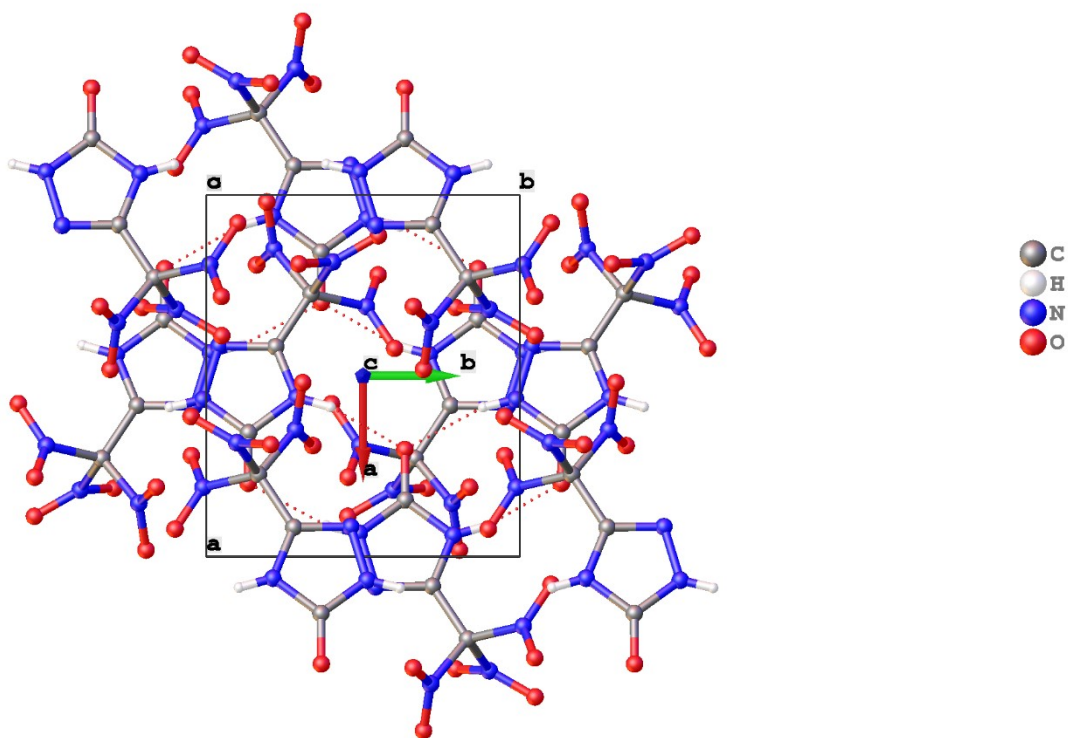


Fig. S9 Packing diagram of TNMTO viewed along the c axis

Table S4: Fractional Atomic Coordinates ($\times 10^4$) and Equivalent Isotropic Displacement Parameters ($\text{\AA}^2 \times 10^3$) for TNMTO. U_{eq} is defined as 1/3 of the trace of the orthogonalised U_{ij} .

Atom	x	y	z	U_{eq}
O1	2032.7(17)	8668.2(19)	2359.4(11)	25.5(4)
O2	5765.4(18)	3997(2)	4271.4(13)	34.2(4)
O3	7798.8(17)	4521(2)	5522.7(12)	30.0(4)
O4	8881.4(18)	4511(2)	3571.0(13)	31.8(4)
O5	8103(3)	7051(3)	2724.6(16)	59.3(7)
O6	8074.7(19)	8398(2)	5643.1(12)	34.2(4)
O7	9816.7(19)	8072(2)	4732.0(15)	38.4(4)
N1	4405(2)	7122(2)	3172.0(13)	23.1(4)
N2	4351(2)	10124(3)	3300.4(14)	24.1(4)
N3	5833(2)	9602(2)	3847.3(14)	25.5(4)
N4	6920(2)	4891(2)	4729.3(14)	26.5(4)
N5	8157(2)	5966(3)	3407.7(15)	32.7(4)
N6	8519(2)	7842(3)	4929.8(15)	28.0(4)
C1	3433(2)	8655(3)	2877.9(16)	23.4(4)
C2	5814(2)	7789(3)	3762.2(16)	23.3(4)
C3	7277(2)	6660(3)	4196.4(16)	25.3(4)

Table S5: Bond Lengths in Å for TNMTO.

Atom	Atom	Length/Å
O1	C1	1.238(3)
O2	N4	1.216(2)
O3	N4	1.206(2)
O4	N5	1.200(2)
O5	N5	1.216(3)
O6	N6	1.207(3)
O7	N6	1.208(2)
N1	C1	1.373(3)
N1	C2	1.368(3)
N2	N3	1.361(2)
N2	C1	1.355(3)
N3	C2	1.297(3)
N4	C3	1.528(3)
N5	C3	1.545(3)
N6	C3	1.535(3)
C2	C3	1.484(3)

Table S6: Bond Angles in ° for TNMTO.

Atom	Atom	Atom	Angle/°
C2	N1	C1	106.41(17)
C1	N2	N3	113.16(17)
C2	N3	N2	103.42(16)
O2	N4	C3	113.98(17)
O3	N4	O2	127.85(19)
O3	N4	C3	118.16(17)
O4	N5	O5	128.3(2)
O4	N5	C3	117.07(18)
O5	N5	C3	114.42(18)
O6	N6	O7	128.3(2)
O6	N6	C3	115.19(17)
O7	N6	C3	116.49(19)
O1	C1	N1	127.48(19)
O1	C1	N2	128.54(19)
N2	C1	N1	103.97(17)
N1	C2	C3	125.92(18)
N3	C2	N1	113.01(17)
N3	C2	C3	120.78(18)
N4	C3	N5	105.24(16)
N4	C3	N6	108.38(16)
N6	C3	N5	105.88(16)
C2	C3	N4	113.67(17)
C2	C3	N5	112.59(18)
C2	C3	N6	110.62(17)

Table S7: Torsion Angles in ° for TNMTO.

Atom	Atom	Atom	Atom	Angle/°
O2	N4	C3	N5	-78.3(2)
O2	N4	C3	N6	168.83(17)
O2	N4	C3	C2	45.4(2)
O3	N4	C3	N5	100.4(2)
O3	N4	C3	N6	-12.5(2)
O3	N4	C3	C2	-135.9(2)
O4	N5	C3	N4	-25.9(2)
O4	N5	C3	N6	88.8(2)
O4	N5	C3	C2	-150.24(19)
O5	N5	C3	N4	158.6(2)
O5	N5	C3	N6	-86.7(2)
O5	N5	C3	C2	34.3(3)
O6	N6	C3	N4	-62.5(2)
O6	N6	C3	N5	-175.03(17)
O6	N6	C3	C2	62.7(2)
O7	N6	C3	N4	116.32(19)
O7	N6	C3	N5	3.8(2)
O7	N6	C3	C2	-118.4(2)
N1	C2	C3	N4	-49.9(3)
N1	C2	C3	N5	69.7(3)
N1	C2	C3	N6	-172.09(19)
N2	N3	C2	N1	1.2(2)
N2	N3	C2	C3	175.43(19)
N3	N2	C1	O1	178.4(2)
N3	N2	C1	N1	-0.5(2)
N3	C2	C3	N4	136.6(2)
N3	C2	C3	N5	-103.8(2)
N3	C2	C3	N6	14.4(3)
C1	N1	C2	N3	-1.5(2)
C1	N1	C2	C3	-175.4(2)
C1	N2	N3	C2	-0.4(2)
C2	N1	C1	O1	-177.8(2)
C2	N1	C1	N2	1.2(2)

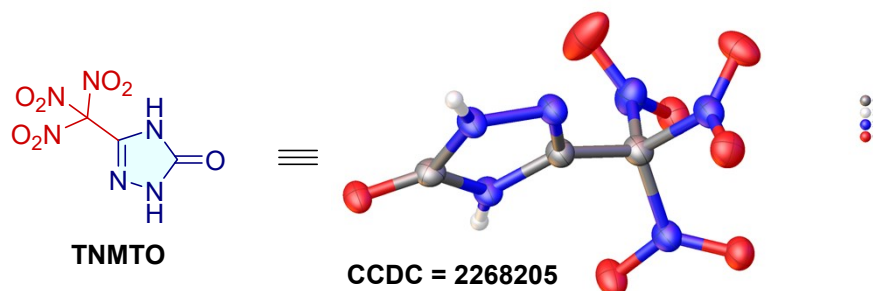
Table S8: Hydrogen Fractional Atomic Coordinates ($\times 10^4$) and Equivalent Isotropic Displacement Parameters ($\text{\AA}^2 \times 10^3$) for TNMTO. U_{eq} is defined as 1/3 of the trace of the orthogonalised U_{ij} .

Atom	x	y	z	U_{eq}
H1	4150(30)	6040(50)	3020(20)	36(8)
H2	4140(30)	11170(50)	3230(20)	33(8)

Table S9: Hydrogen Bond information for TNMTO.

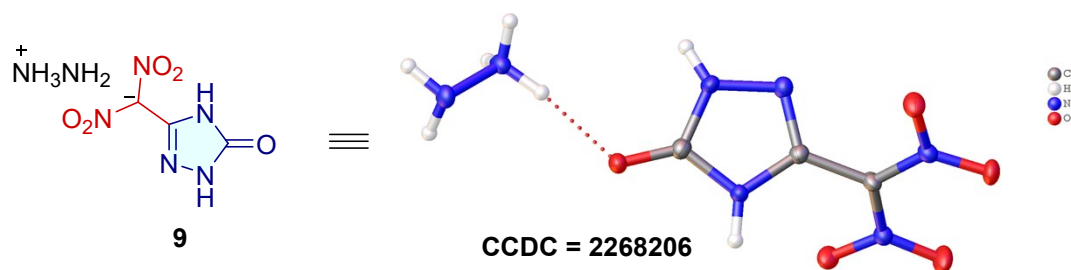
D	H	A	d(D-H)/\AA	d(H-A)/\AA	d(D-A)/\AA	D-H-A/deg
N1	H1	O1 ¹	0.81(3)	1.97(3)	2.770(2)	166(3)
N2	H2	O1 ²	0.77(3)	2.11(3)	2.845(2)	161(3)

¹1/2-x,-1/2+y,1/2-z; ²1/2-x,1/2+y,1/2-z

Table S10. Single crystal X-ray data and structure refinement for TNMTO.⁶⁻¹⁰

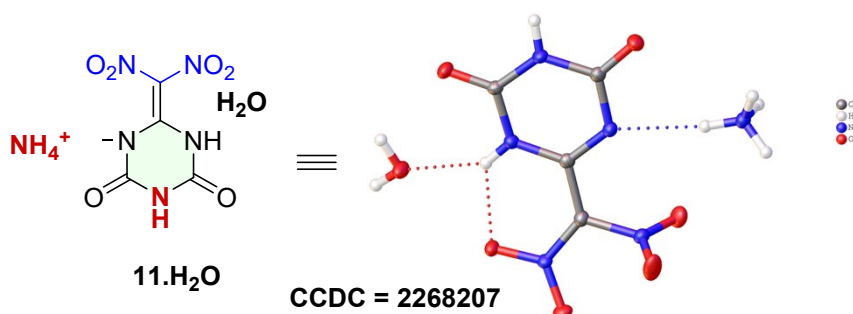
Formula	C ₃ H ₂ N ₆ O ₇ (CCDC = 2268205)
$D_{calc.}/g\ cm^{-3}$	1.902
m/mm^{-1}	1.682
Formula Weight	234.11
Colour	yellow
Shape	needle-shaped
Size/mm ³	0.11×0.04×0.02
T/K	100.00(10)
Crystal System	monoclinic
Space Group	$P2_1/n$
$a/\text{Å}$	8.4982(2)
$b/\text{Å}$	7.1276(2)
$c/\text{Å}$	13.8819(4)
a°	90
b°	103.573(3)
g°	90
$V/\text{Å}^3$	817.37(4)
Z	4
Z'	1
Wavelength/Å	1.54184
Radiation type	Cu K_α
Q_{min}°	5.585
Q_{max}°	80.393
Measured Refl's.	8681
Indep't Refl's	1751
Refl's $I \geq 2\ \sigma(I)$	1461
R_{int}	0.0436
Parameters	153
Restraints	0
Largest Peak	0.488
Deepest Hole	-0.402
GooF	1.055
wR_2 (all data)	0.1356
wR_2	0.1274
R_1 (all data)	0.0551
R_1	0.0459

Table S11. Single crystal X-ray data and structure refinement for compound 9.⁶⁻¹⁰



Formula	C ₃ H ₇ N ₇ O ₅ (CCDC = 2268206)
$D_{calc.}/g\text{ cm}^{-3}$	1.899
μ/mm^{-1}	1.554
Formula Weight	221.16
Colour	yellow
Shape	needle-shaped
Size/ mm^3	0.17×0.02×0.01
T/K	100.15
Crystal System	monoclinic
Space Group	$P2_1/n$
$a/\text{Å}$	3.63691(18)
$b/\text{Å}$	17.1203(9)
$c/\text{Å}$	12.4539(6)
$\alpha/^\circ$	90
$\beta/^\circ$	94.177(4)
$\gamma/^\circ$	90
$V/\text{Å}^3$	773.38(7)
Z	4
Z'	1
Wavelength/ Å	1.54184
Radiation type	Cu K_α
$\theta_{min}/^\circ$	4.398
$\theta_{max}/^\circ$	81.103
Measured Refl's.	8241
Indep't Refl's	1657
Refl's $I \geq 2\sigma(I)$	1318
R_{int}	0.0797
Parameters	164
Restraints	0
Largest Peak	0.325
Deepest Hole	-0.318
Goof	1.077
wR_2 (all data)	0.1229
wR_2	0.1107
R_1 (all data)	0.0623
R_1	0.0452

Table S12. Single crystal X-ray data and structure refinement for compound 11.H₂O.⁶⁻¹⁰



Formula	C ₄ H ₈ N ₆ O ₇ (CCDC = 2268207)
$D_{calc.}/\text{g cm}^{-3}$	1.788
m/mm^{-1}	1.507
Formula Weight	252.16
Colour	yellow
Shape	block-shaped
Size/ mm^3	0.11×0.07×0.06
T/K	100.00(10)
Crystal System	monoclinic
Flack Parameter	0.6(4)
Hooft Parameter	0.2(2)
Space Group	<i>Ia</i>
$a/\text{Å}$	8.26070(10)
$b/\text{Å}$	9.13530(10)
$c/\text{Å}$	12.5011(2)
a°	90
b°	96.6790(10)
g°	90
$V/\text{Å}^3$	936.98(2)
Z	4
Z'	1
Wavelength/Å	1.54184
Radiation type	Cu K _{α}
Q_{min}°	6.014
Q_{max}°	80.141
Measured Refl's.	5189
Indep't Refl's	1465
Refl's $I \geq 2\sigma(I)$	1424
R_{int}	0.0309
Parameters	187
Restraints	2
Largest Peak	0.148
Deepest Hole	-0.218
GooF	1.065
wR_2 (all data)	0.0765
wR_2	0.0756
R_1 (all data)	0.0295
R_1	0.0286

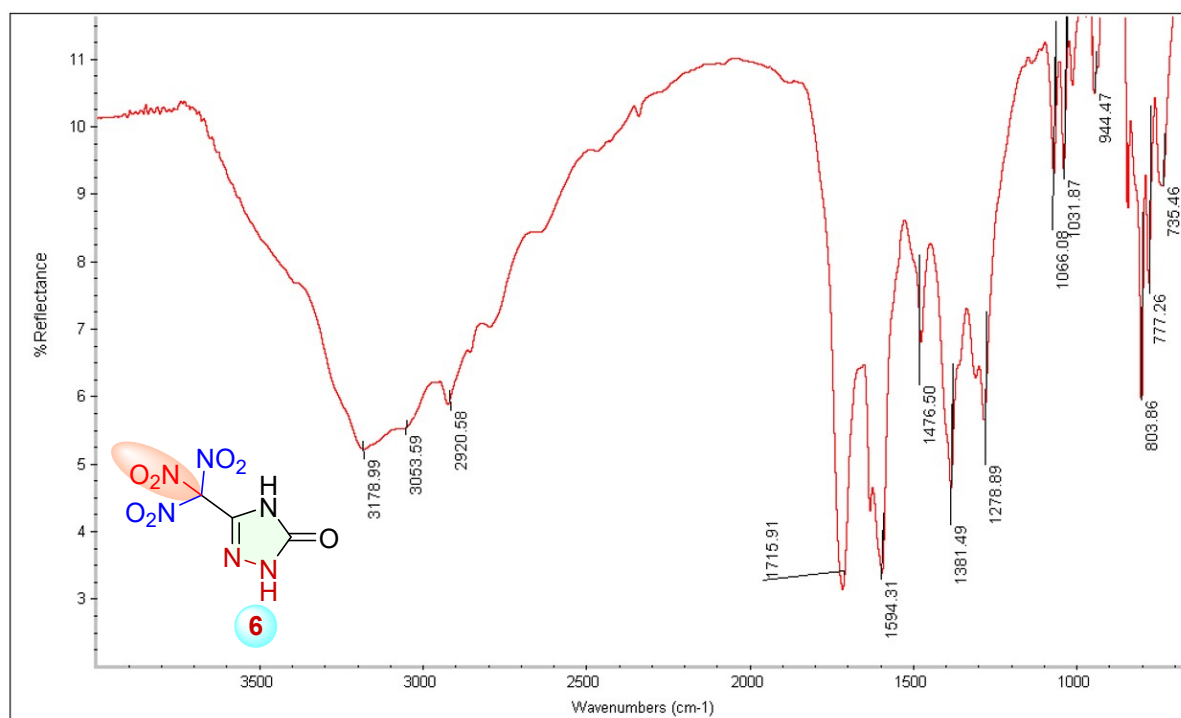


Fig. S10 FTIR-Spectrum of Compound 6.

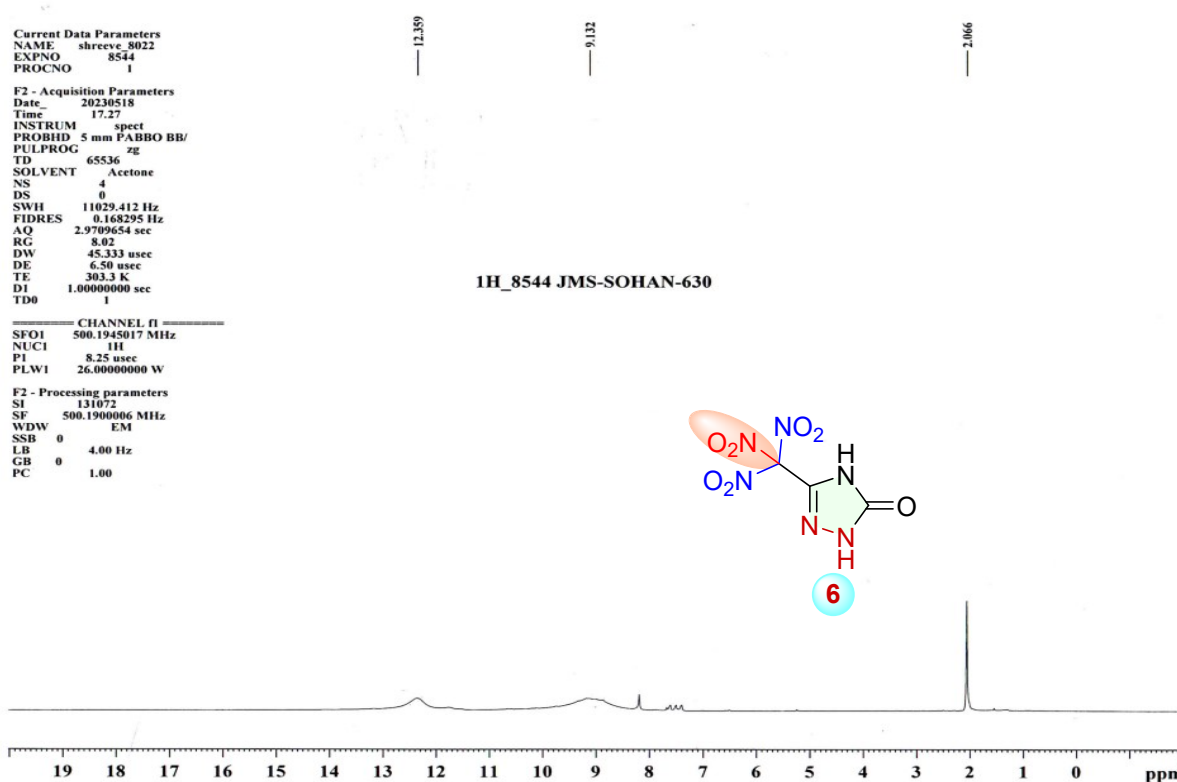


Fig. S11 ¹H NMR Spectrum of Compound 6 (500.19 MHz).

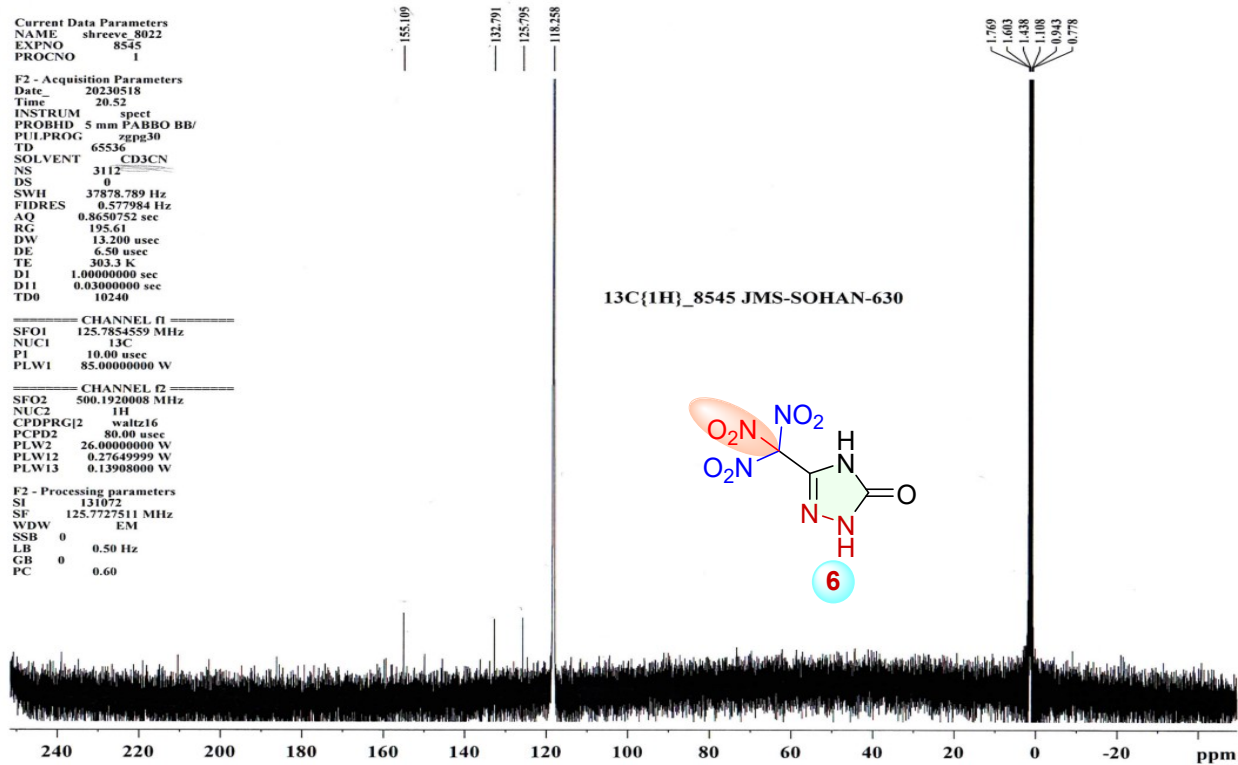


Fig. S12 ¹³C NMR Spectrum of Compound 6 (125.77 MHz).

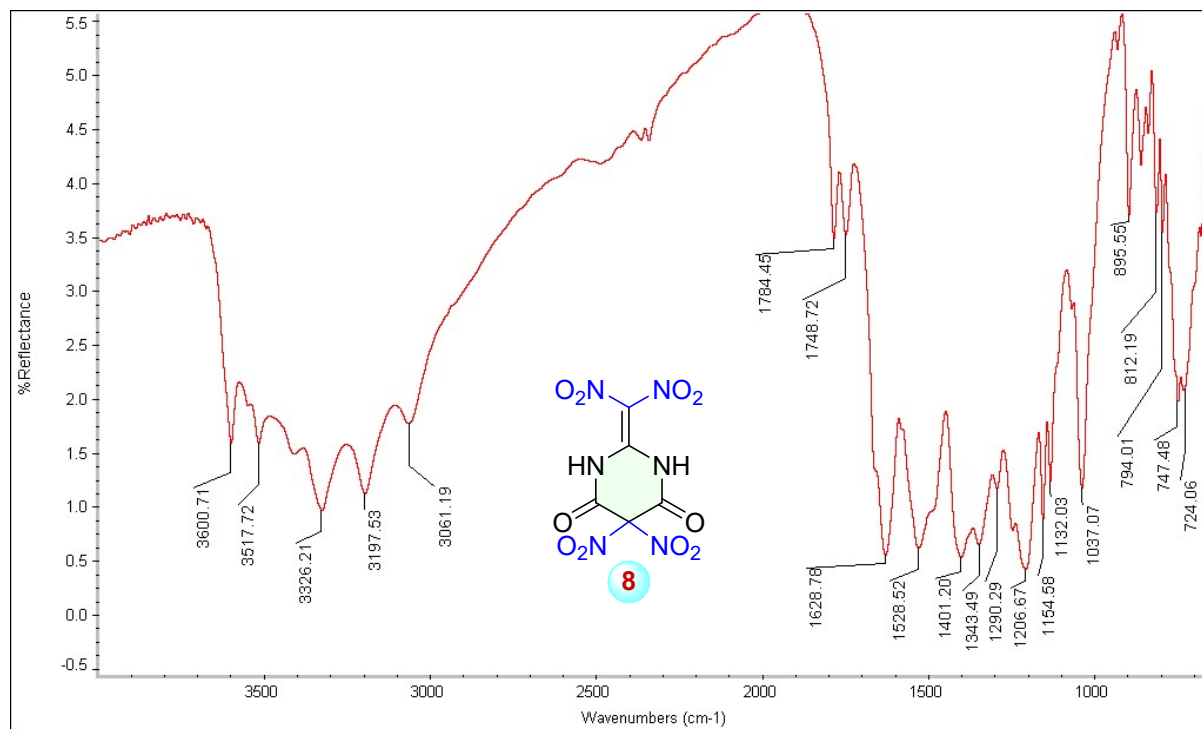


Fig. S13 FTIR-Spectrum of Compound 8.

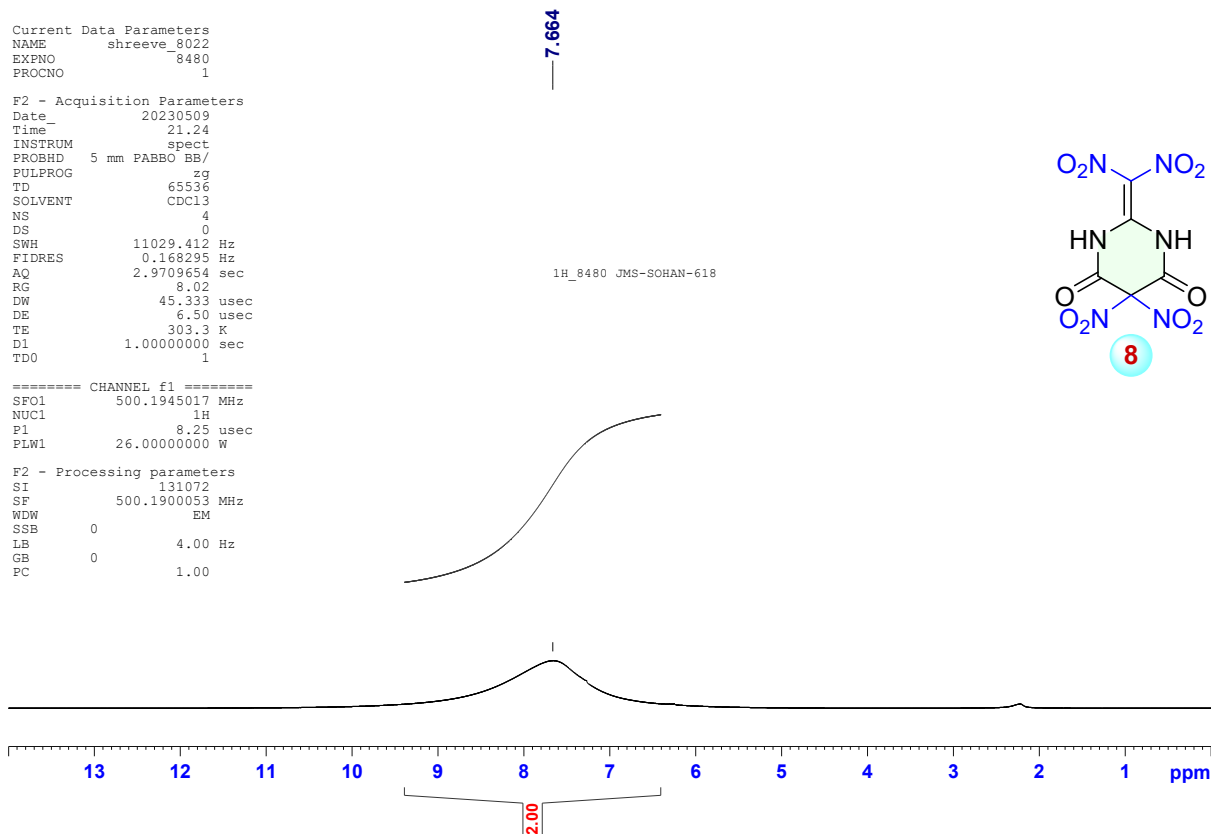


Fig. S14 ¹H NMR Spectrum of Compound 8 (500.19 MHz).

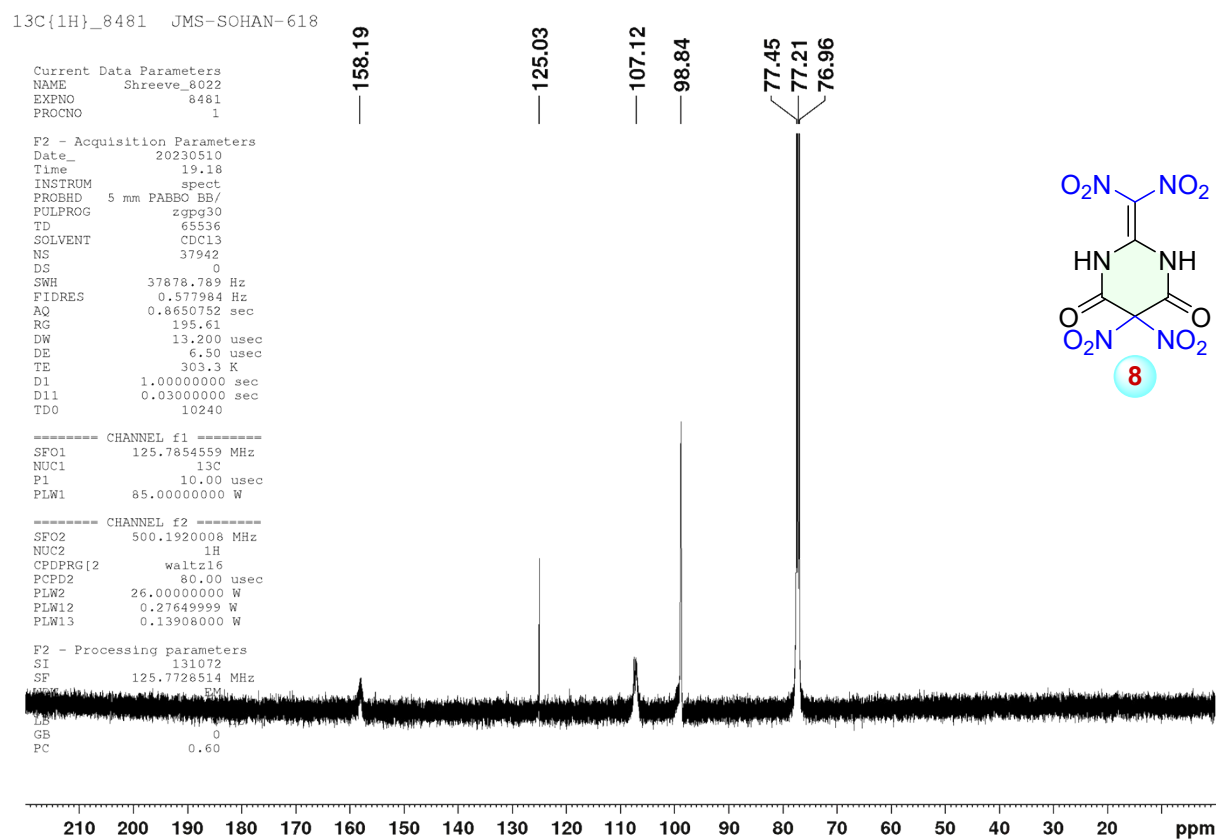


Fig. S15 ¹³C NMR Spectrum of Compound 8 (125.77 MHz).

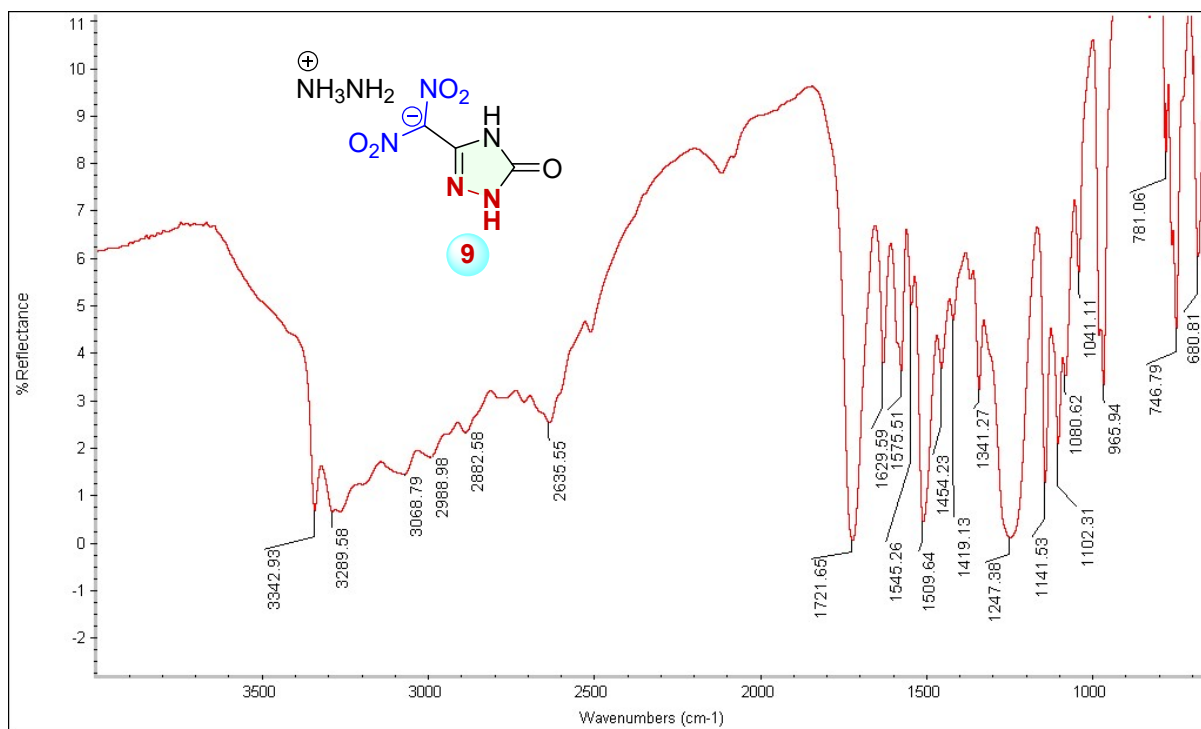


Fig. S16 FTIR-Spectrum of Compound 9.

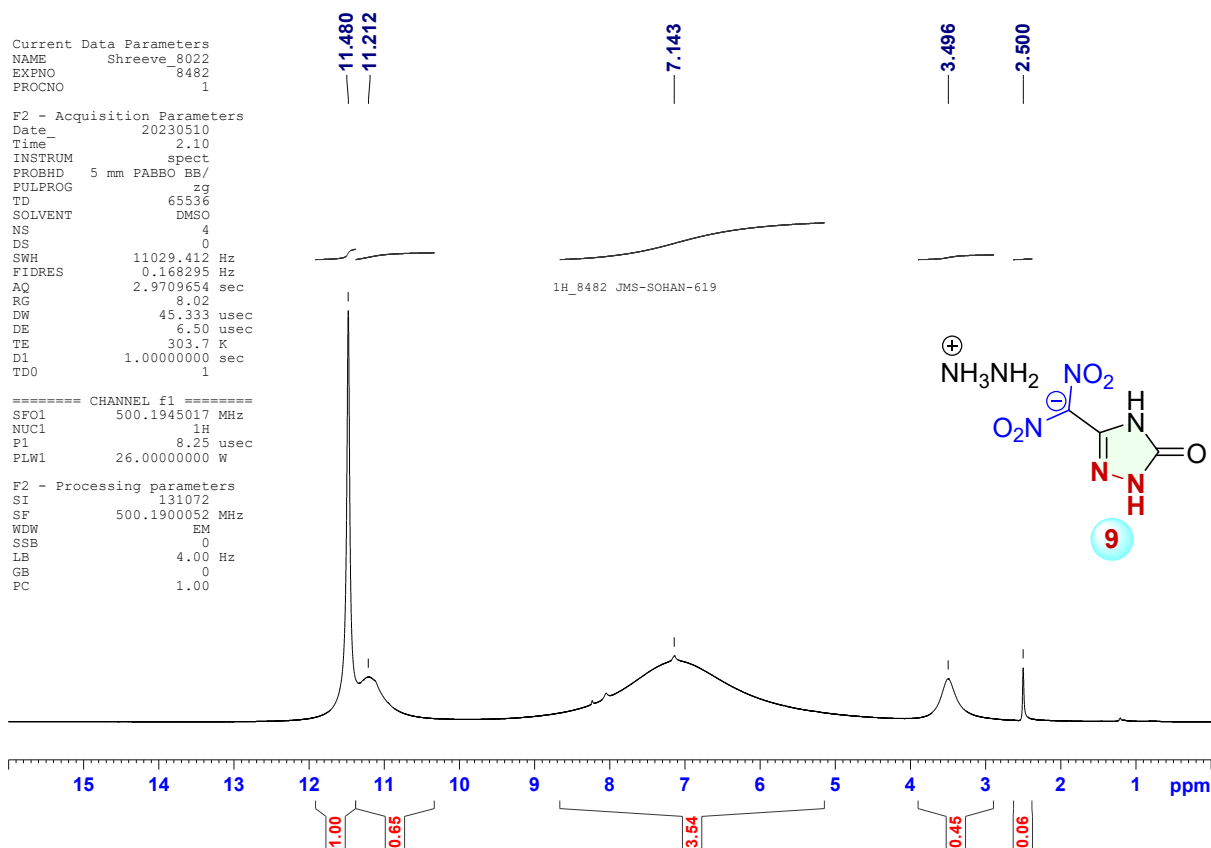


Fig. S17 ¹H NMR Spectrum of Compound 9 (500.19 MHz).

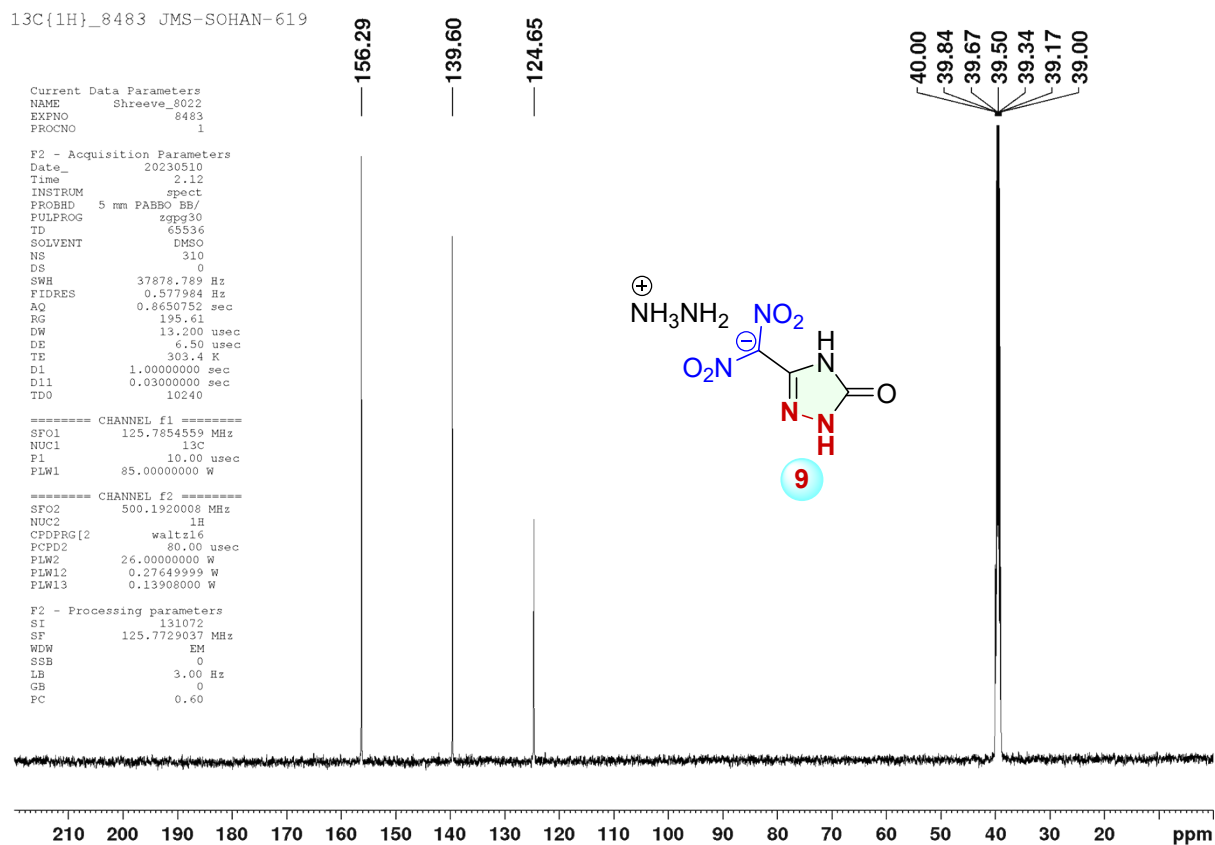


Fig. S18 ¹³C NMR Spectrum of Compound 9 (125.77 MHz).

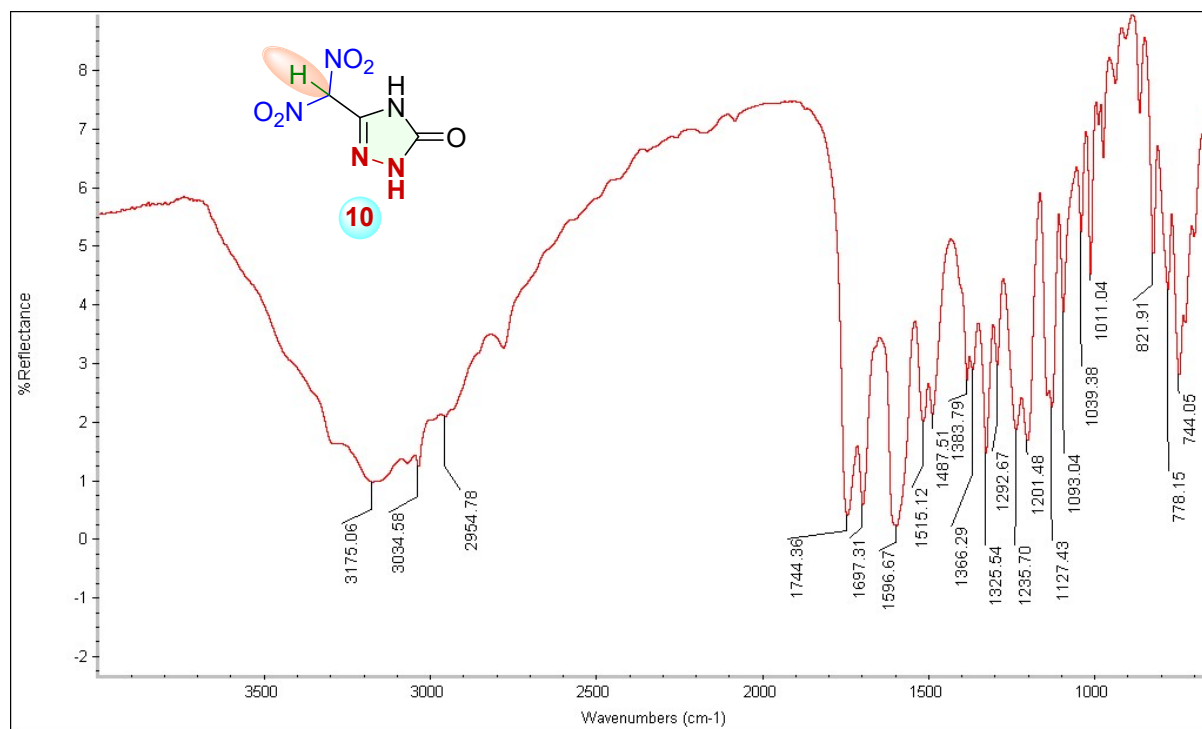


Fig. S19 FTIR-Spectrum of Compound 10.

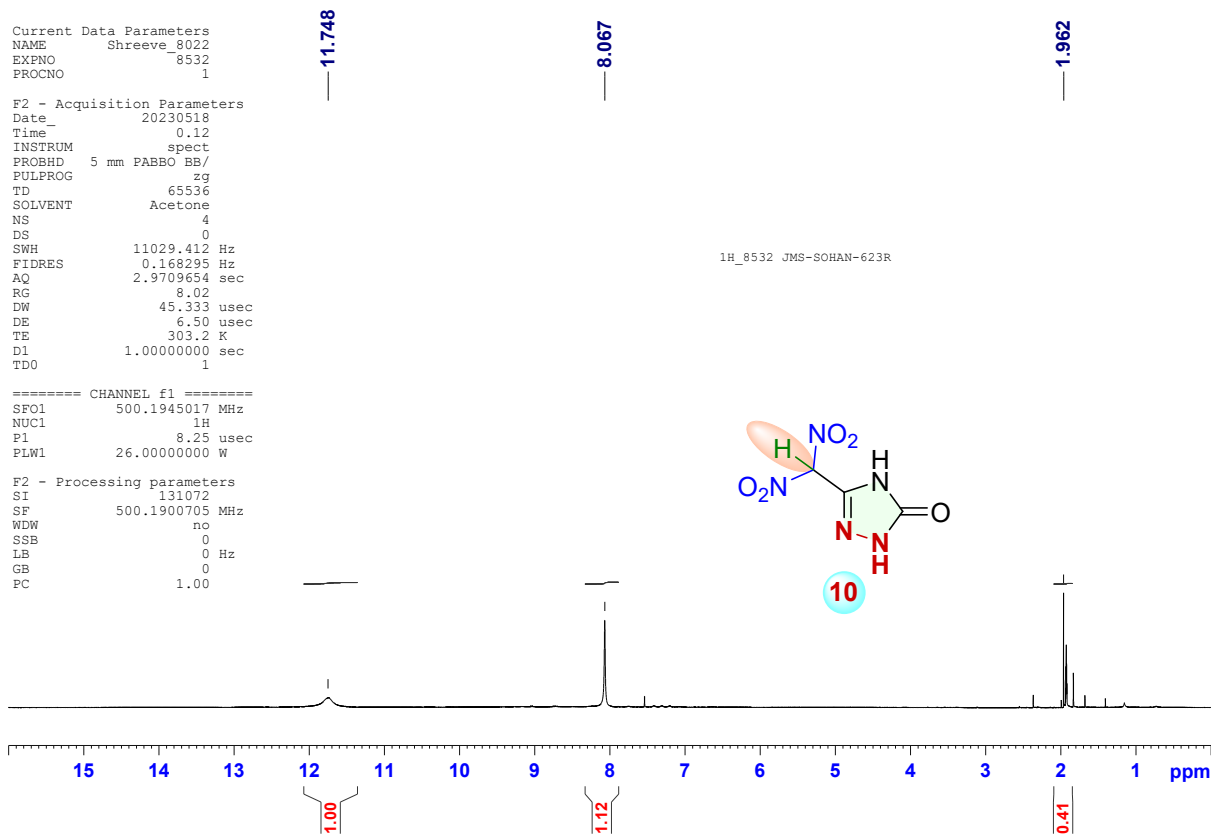


Fig. S20 ¹H NMR Spectrum of Compound 10 (500.19 MHz).

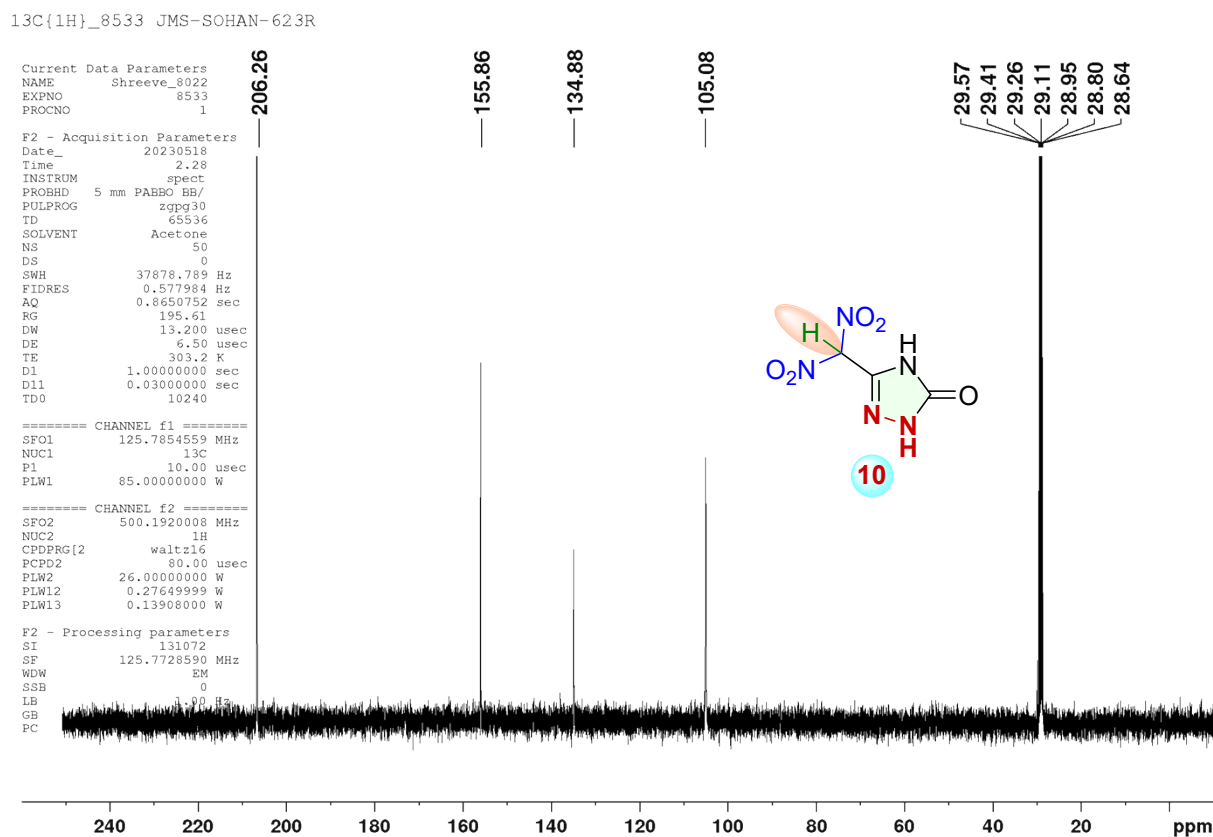


Fig. S21 ¹³C NMR Spectrum of Compound 10 (125.77 MHz).

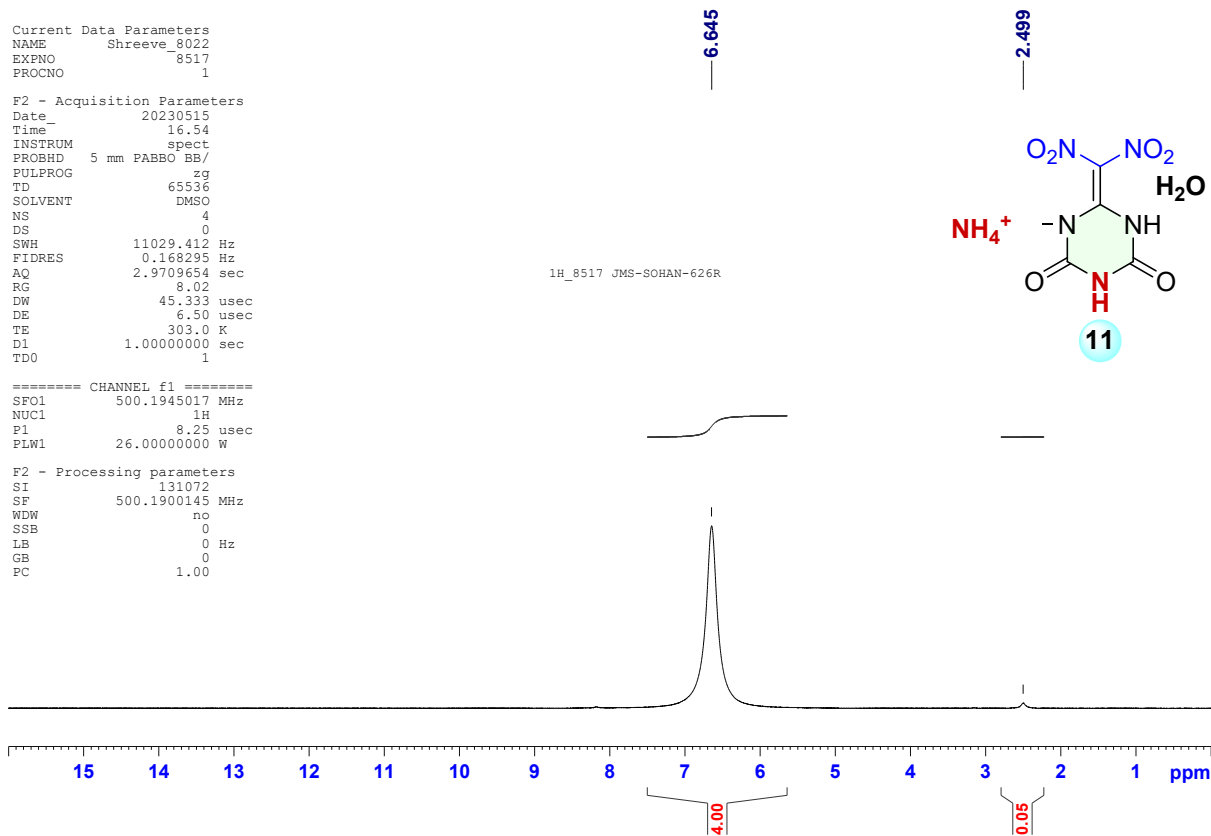


Fig. S22 ¹H NMR Spectrum of Compound 11.H₂O (500.19 MHz).

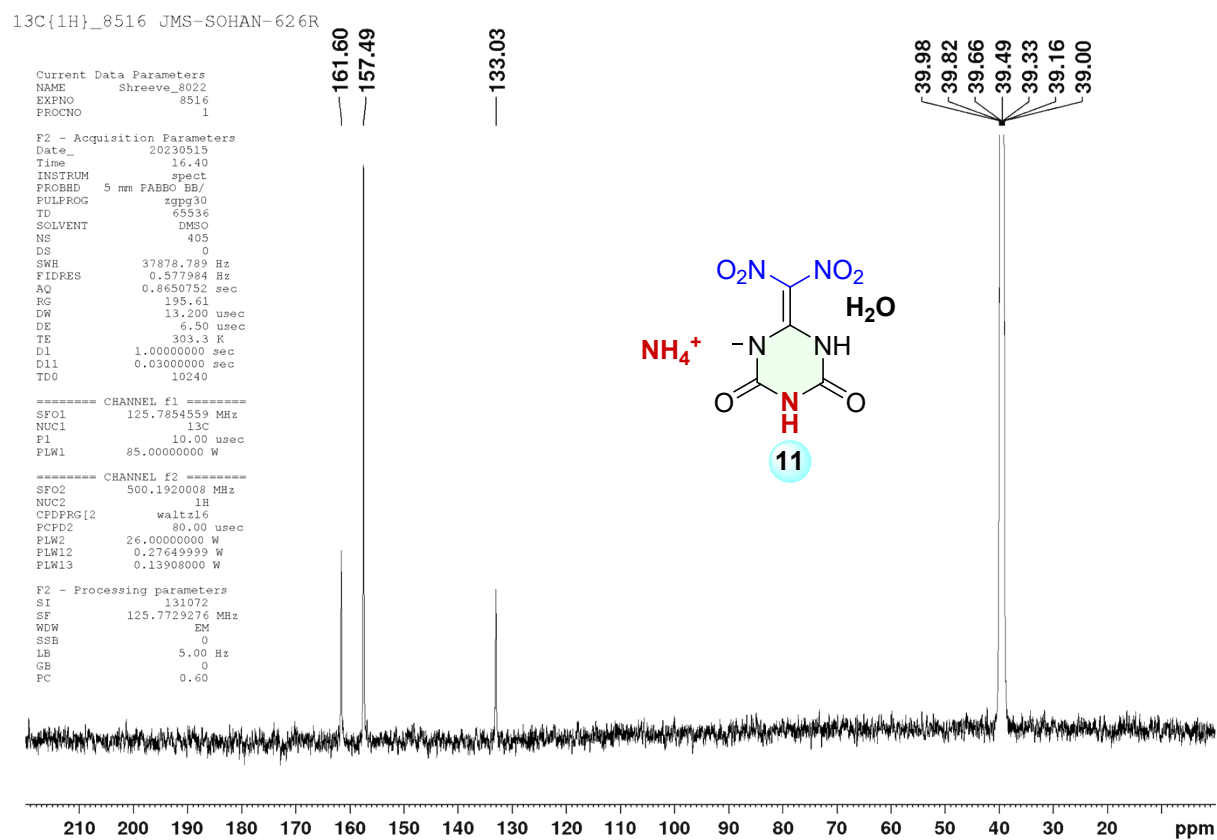


Fig. S23 ¹³C NMR Spectrum of Compound 11.H₂O (125.77 MHz).

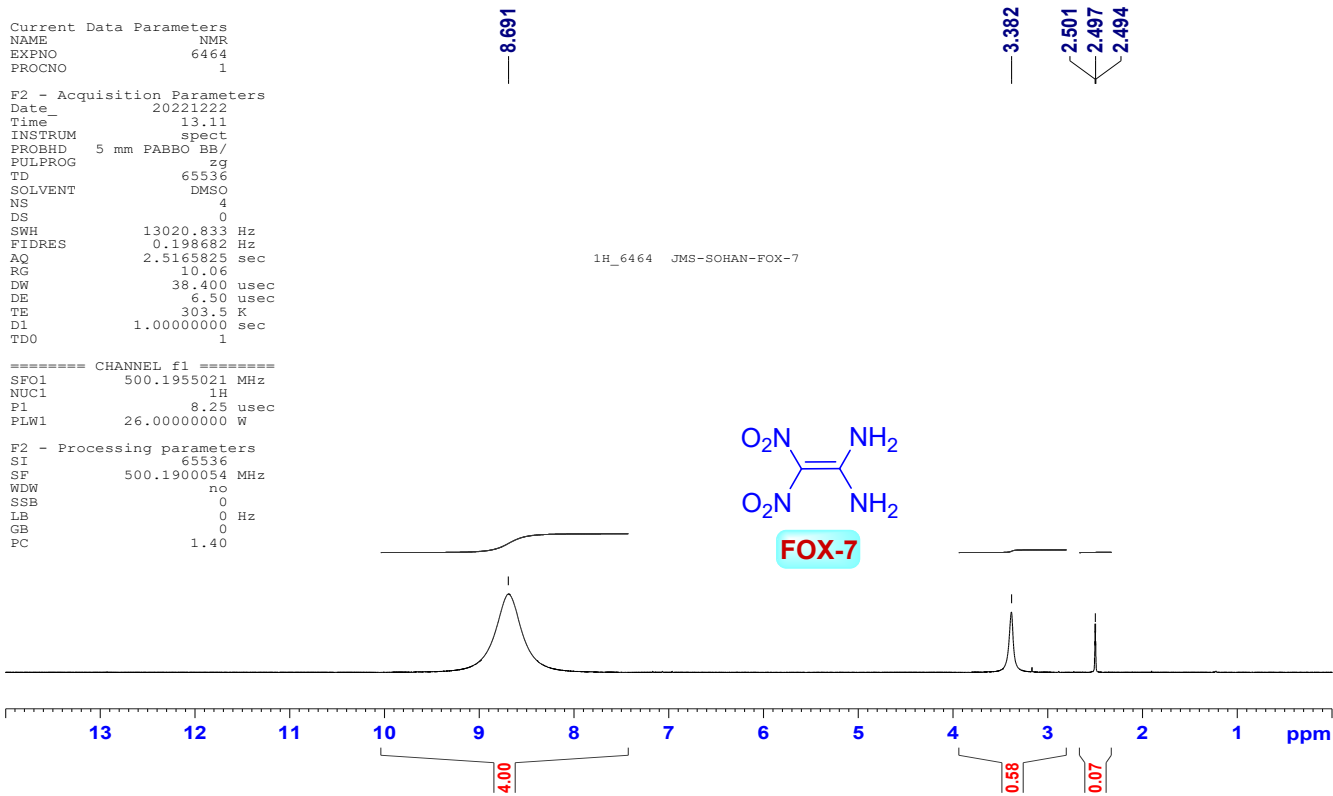


Fig. S24 ¹H NMR Spectrum of FOX-7 (500.19 MHz).

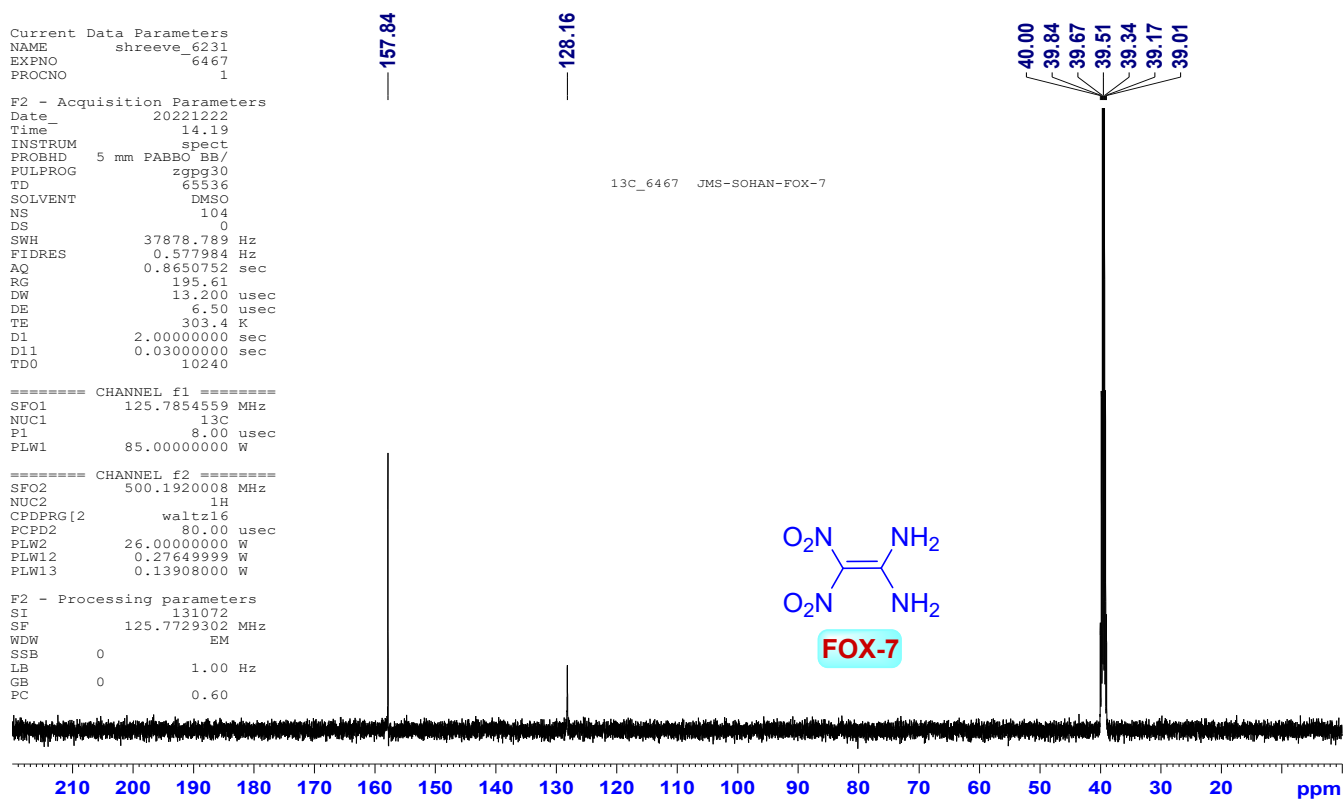


Fig. S25 ¹³C NMR Spectrum of FOX-7 (125.77 MHz).

Sample: SOHAN-630 R at 5°C
Size: 0.1000 mg
Method: Ramp

DSC

File: C:\DSC\SOHAN\SOHAN-630 R at 5°C.002
Operator: SOHAN
Run Date: 05-Jun-2023 00:06
Instrument: DSC Q2000 V24.11 Build 124

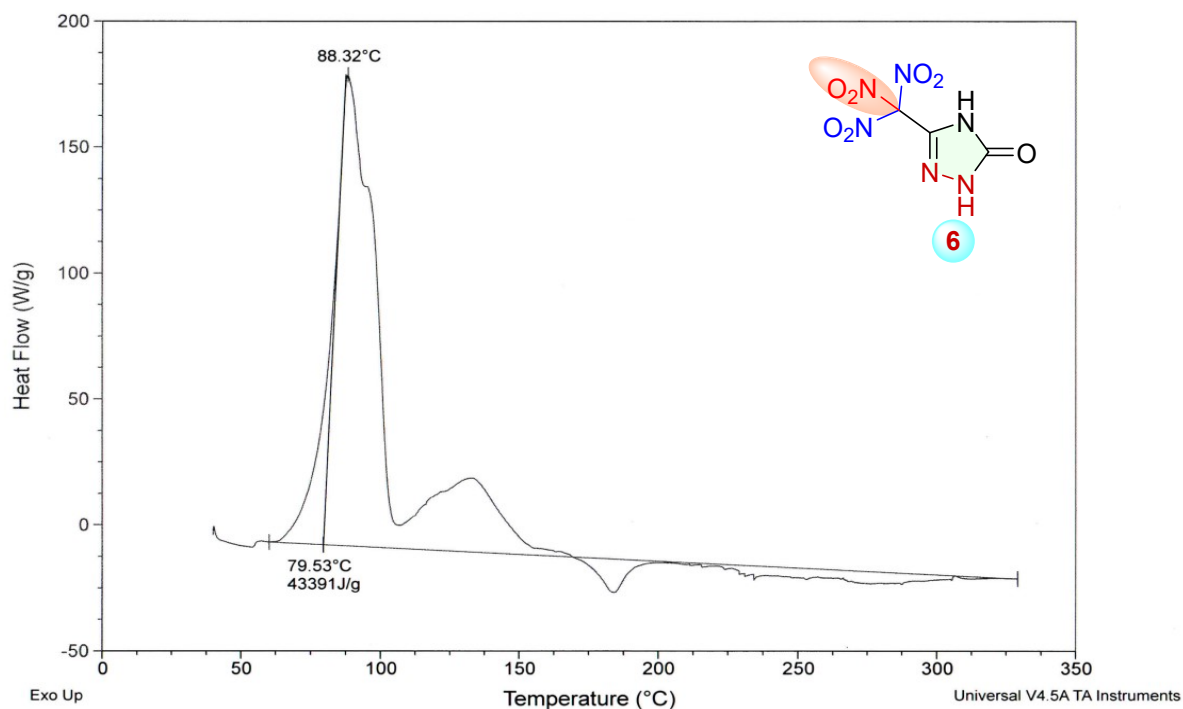


Fig. S26 DSC of compound 6 at 5 °C min⁻¹

Sample: SOHAN-630RRR at 10°C
Size: 0.1000 mg
Method: Ramp

DSC

File: C:\DSC\SOHAN\SOHAN-630RRR at 10°C.C
Operator: SOHAN
Run Date: 25-May-2023 11:04
Instrument: DSC Q2000 V24.11 Build 124

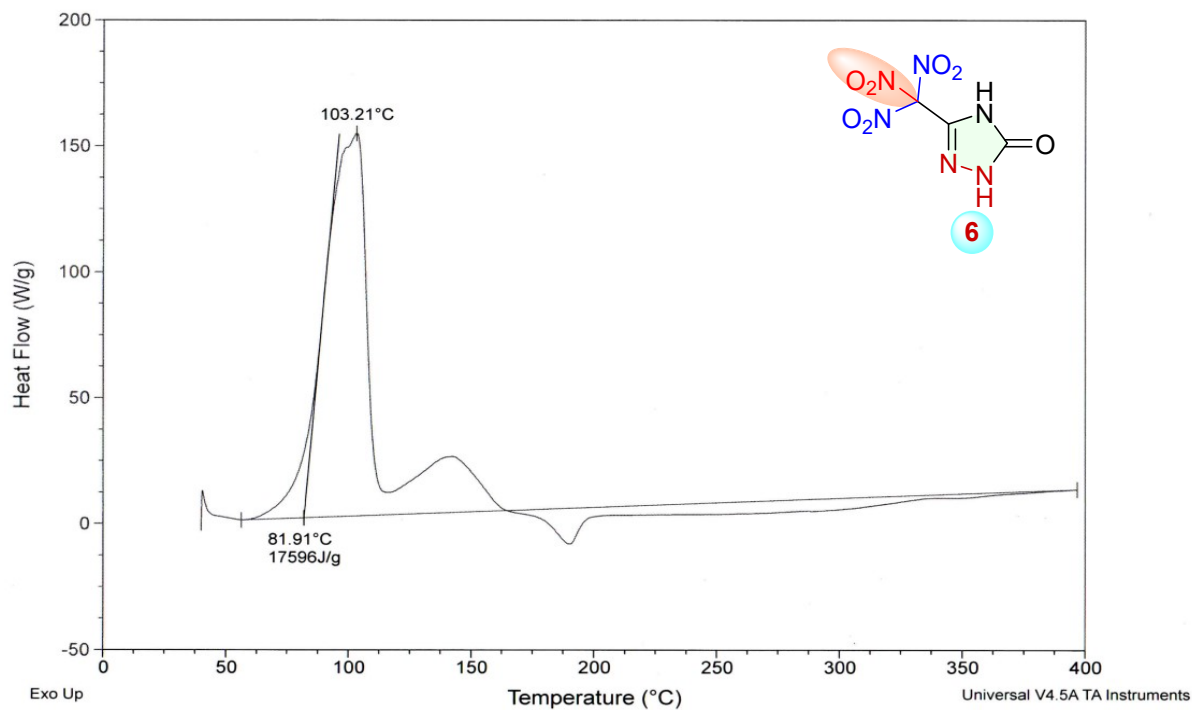


Fig. S27 DSC of compound 6 at 10 °C min⁻¹

Sample: SOHAN-618R at 5°C
Size: 0.1000 mg
Method: Ramp

DSC

File: C:\DSC\SOHAN\SOHAN-618R at 5°C.001
Operator: SOHAN
Run Date: 09-May-2023 22:32
Instrument: DSC Q2000 V24.11 Build 124

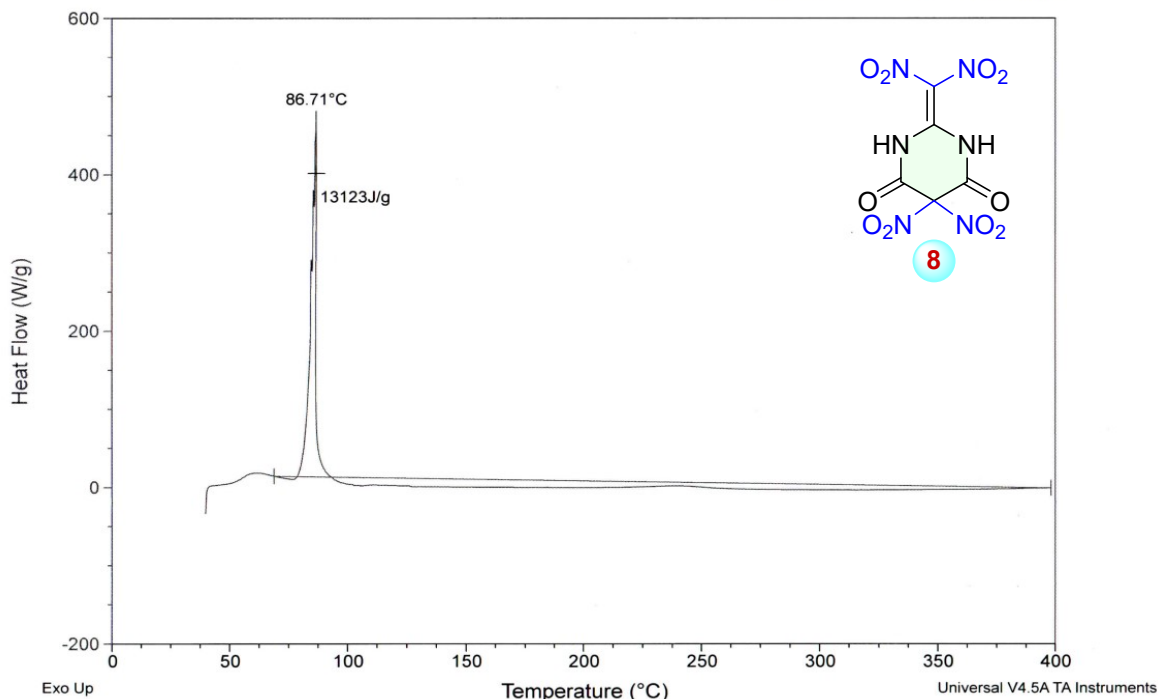


Fig. S28 DSC of compound 8 at 5 °C min⁻¹

Sample: SOHAN-618R at 10°C
Size: 0.1000 mg
Method: Ramp

DSC

File: C:\DSC\SOHAN\SOHAN-618R at 10°C.001
Operator: SOHAN
Run Date: 09-May-2023 21:44
Instrument: DSC Q2000 V24.11 Build 124

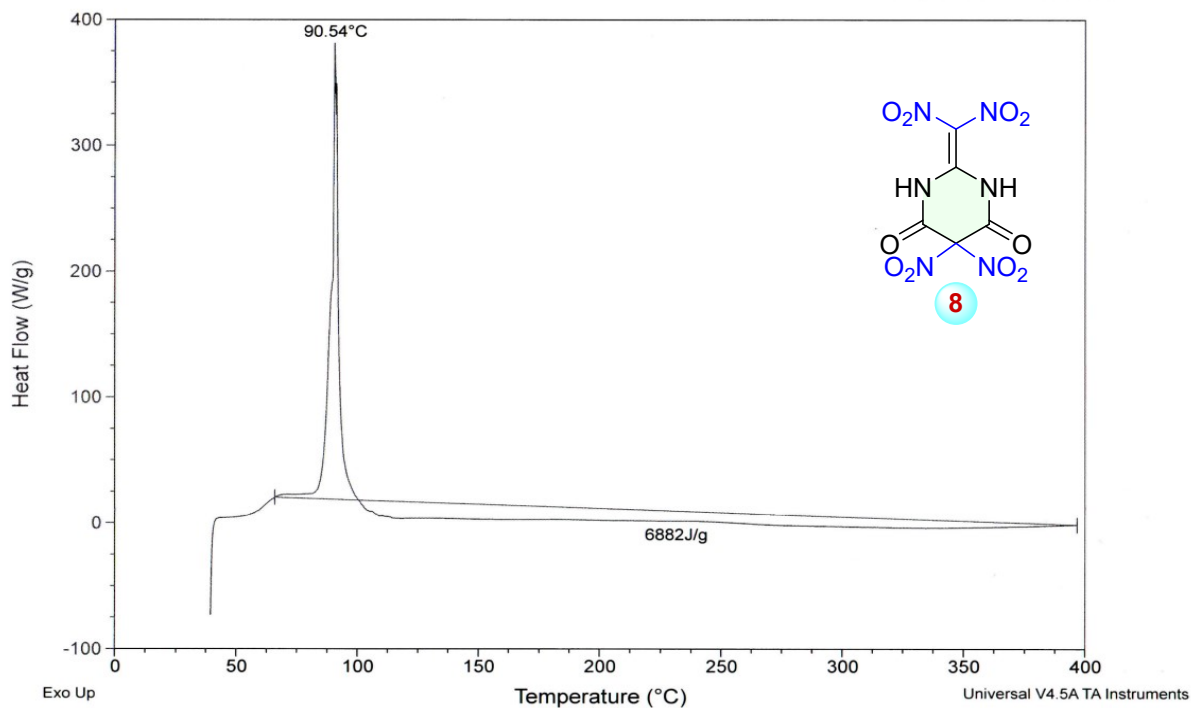


Fig. S29 DSC of compound 8 at 10 °C min⁻¹

Sample: SOHAN-619 at 5°C
Size: 0.1000 mg
Method: Ramp

DSC

File: C:\DSC\SOHAN\SOHAN-619 at 5°C.001
Operator: SOHAN
Run Date: 10-May-2023 11:03
Instrument: DSC Q2000 V24.11 Build 124

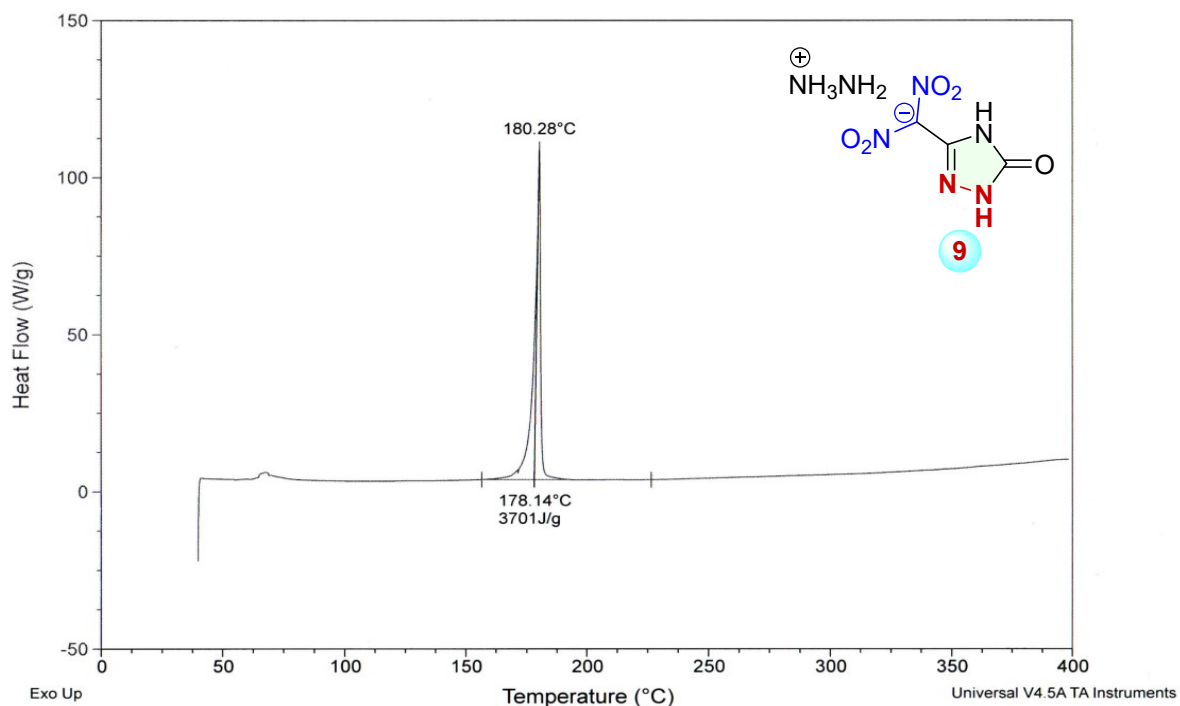


Fig. S30 DSC of compound 9 at 5 °C min⁻¹

Sample: SOHAN-619 at 10°C
Size: 0.1000 mg
Method: Ramp

DSC

File: C:\DSC\SOHAN\SOHAN-619 at 10°C.001
Operator: SOHAN
Run Date: 10-May-2023 00:01
Instrument: DSC Q2000 V24.11 Build 124

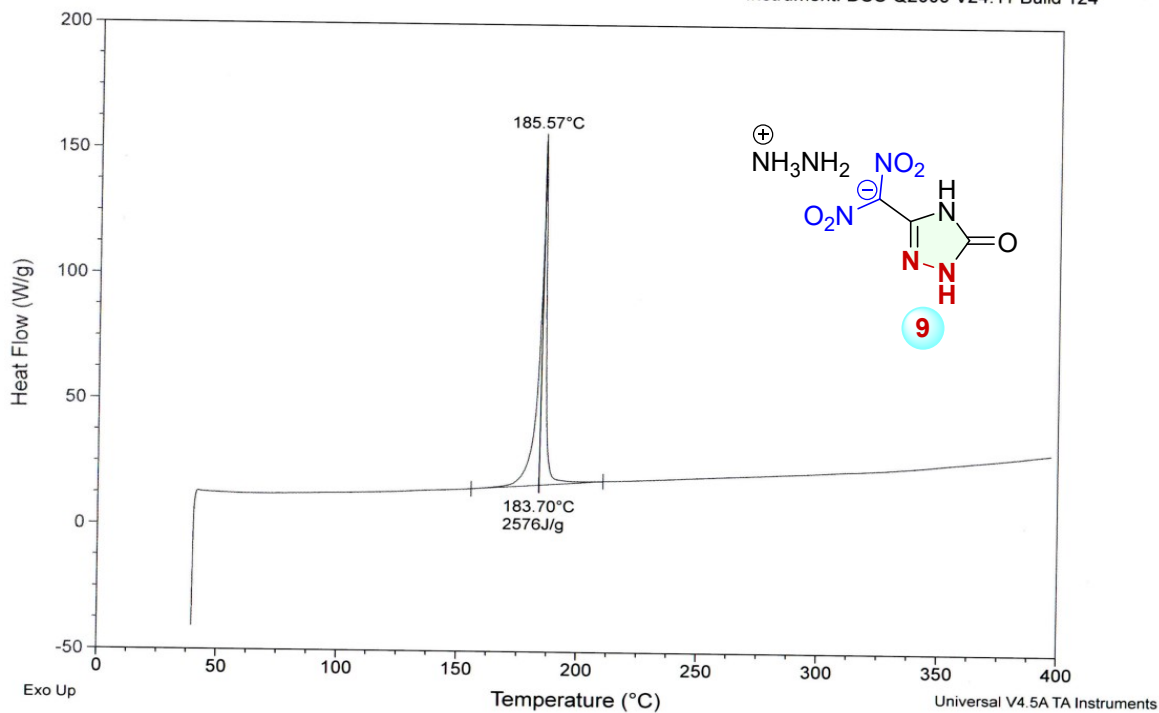


Fig. S31 DSC of compound 8 at 10 °C min⁻¹

Sample: SOHAN-623RR at 5°C
Size: 0.1000 mg
Method: Ramp

DSC

File: C:\...\DSC\SOHAN\SOHAN-623RR at 5°C.001
Operator: SOHAN
Run Date: 23-May-2023 17:25
Instrument: DSC Q2000 V24.11 Build 124

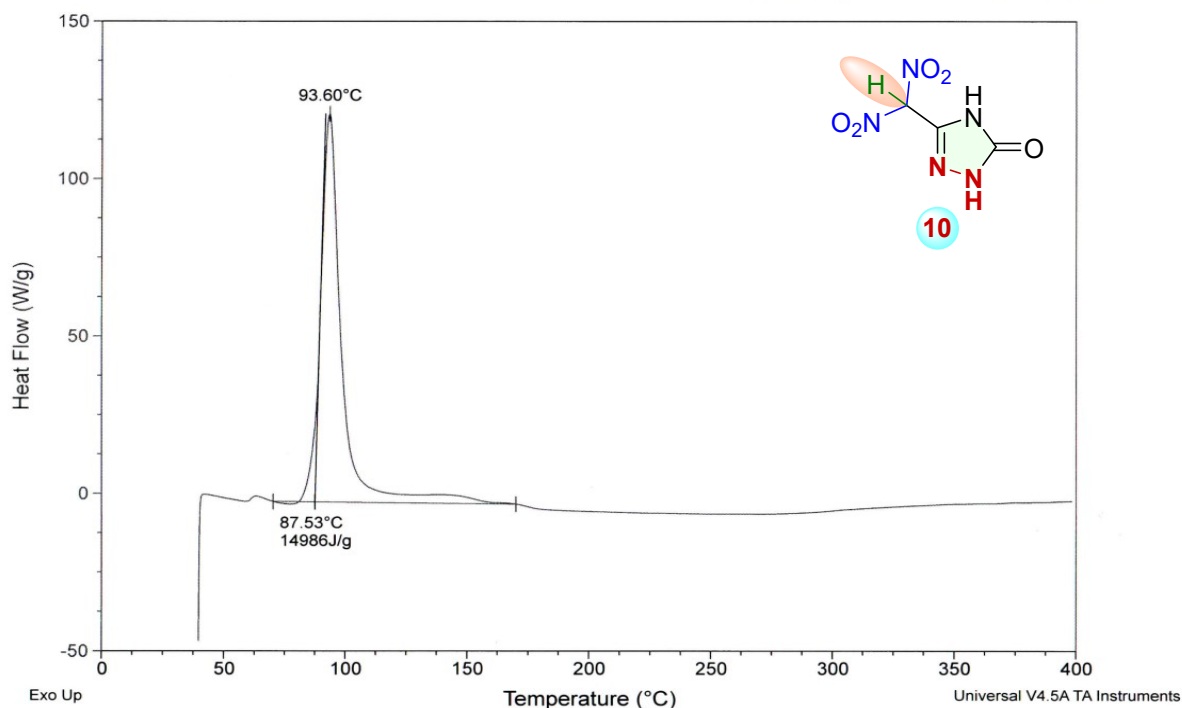


Fig. S32 DSC of compound 10 at 5 °C min⁻¹

Sample: SOHAN-623RR at 10°C
Size: 0.1000 mg
Method: Ramp

DSC

File: C:\...\DSC\SOHAN\SOHAN-623RR at 10°C.00
Operator: SOHAN
Run Date: 23-May-2023 20:24
Instrument: DSC Q2000 V24.11 Build 124

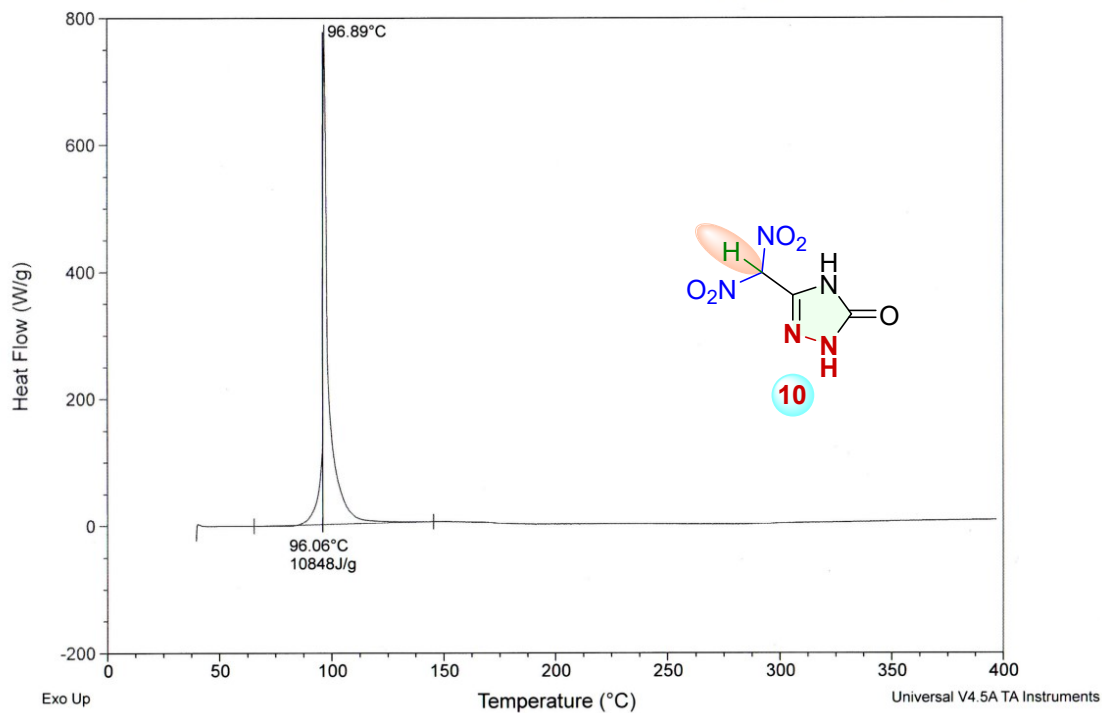


Fig. S33 DSC of compound 10 at 10 °C min⁻¹

Sample: SOHAN-626R at 5°C
Size: 0.1000 mg
Method: Ramp

DSC

File: C:\DSC\SOHAN\SOHAN-626R at 5°C.001
Operator: SOHAN
Run Date: 06-Jun-2023 17:28
Instrument: DSC Q2000 V24.11 Build 124

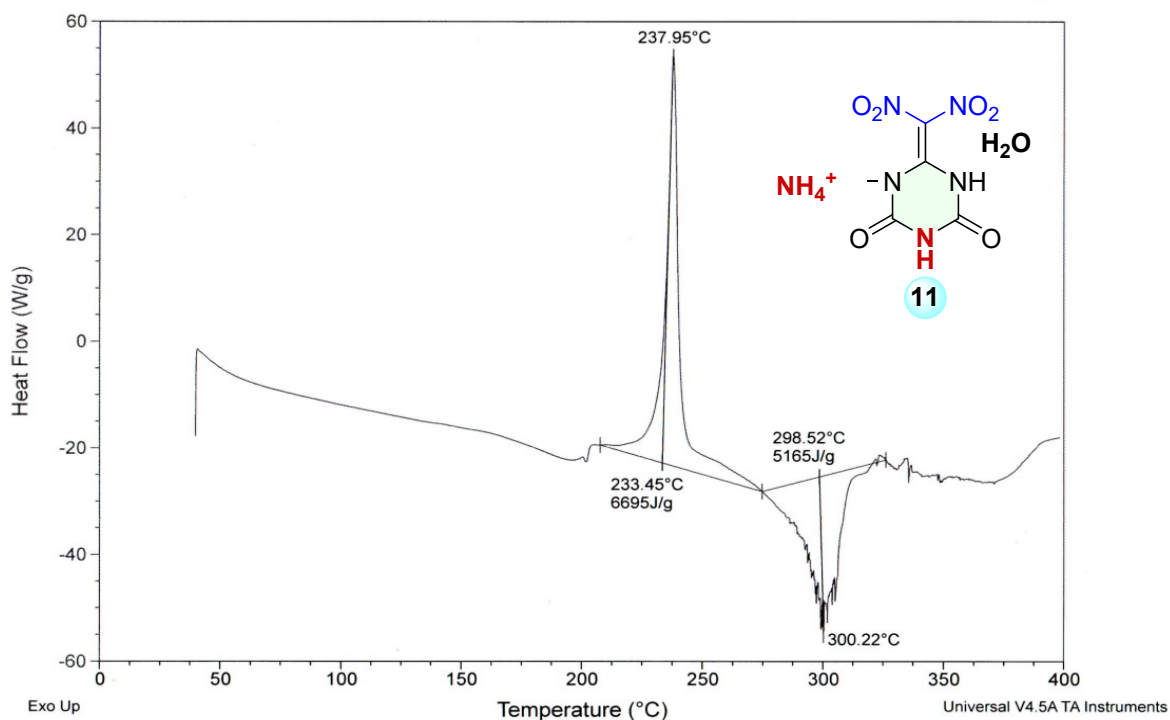


Fig. S34 DSC of compound 11.H₂O at 5 °C min⁻¹

Sample: SOHAN-FOX-7 at 5°C
Size: 0.1000 mg
Method: Ramp
Comment: Cell constant calibration

DSC

File: C:\DSC\SOHAN\SOHAN-FOX-7 at 5°C.001
Operator: SOHAN
Run Date: 19-Dec-2022 17:52
Instrument: DSC Q2000 V24.11 Build 124

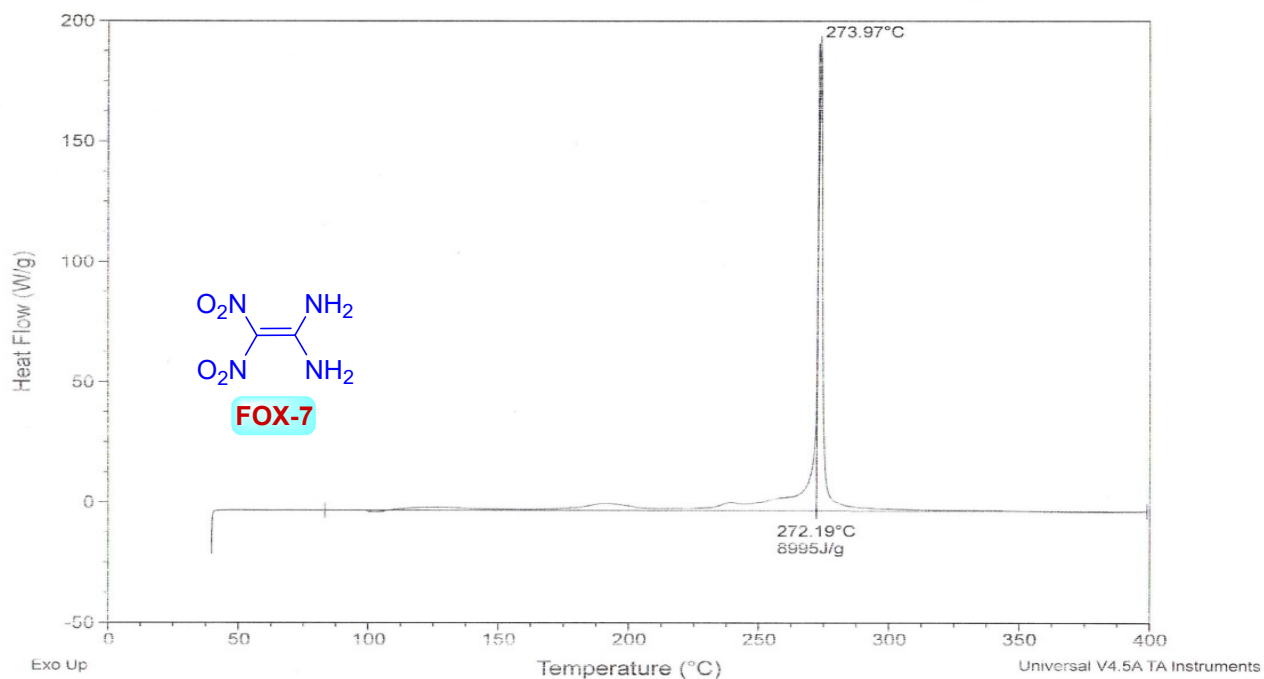


Fig. S35 DSC of compound FOX-7 at 5 °C min⁻¹

Sample: SOHAN-630 at 5°C
Size: 2.6780 mg
Method: Ramp

TGA

File: C:\...TGA\Sohan\SOHAN-630 at 5°C.001
Operator: SOHAN
Run Date: 05-Jun-2023 00:38
Instrument: TGA Q50 V20.13 Build 39

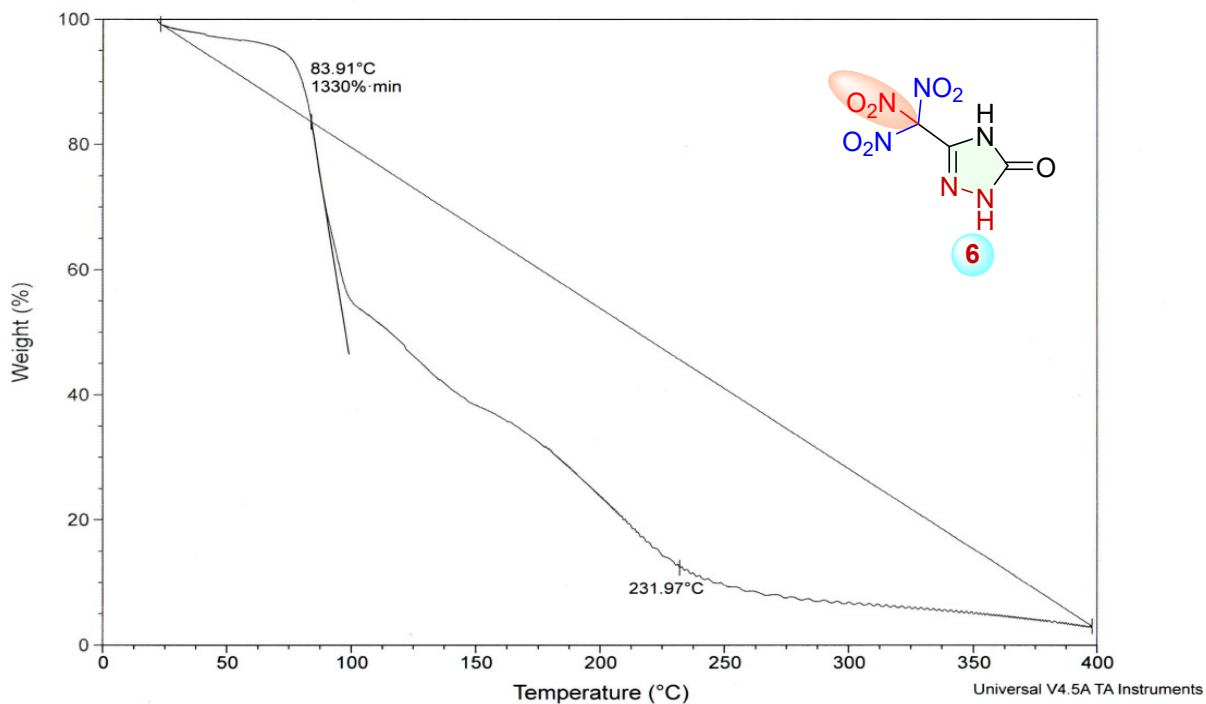


Fig. S36 TGA of compound 6 at 5 °C min⁻¹

Sample: SOHAN-618R at 5°C
Size: 2.1190 mg
Method: Ramp

TGA

File: C:\...TGA\Sohan\SOHAN-618R at 5°C.001
Operator: SOHAN
Run Date: 09-May-2023 22:53
Instrument: TGA Q50 V20.13 Build 39

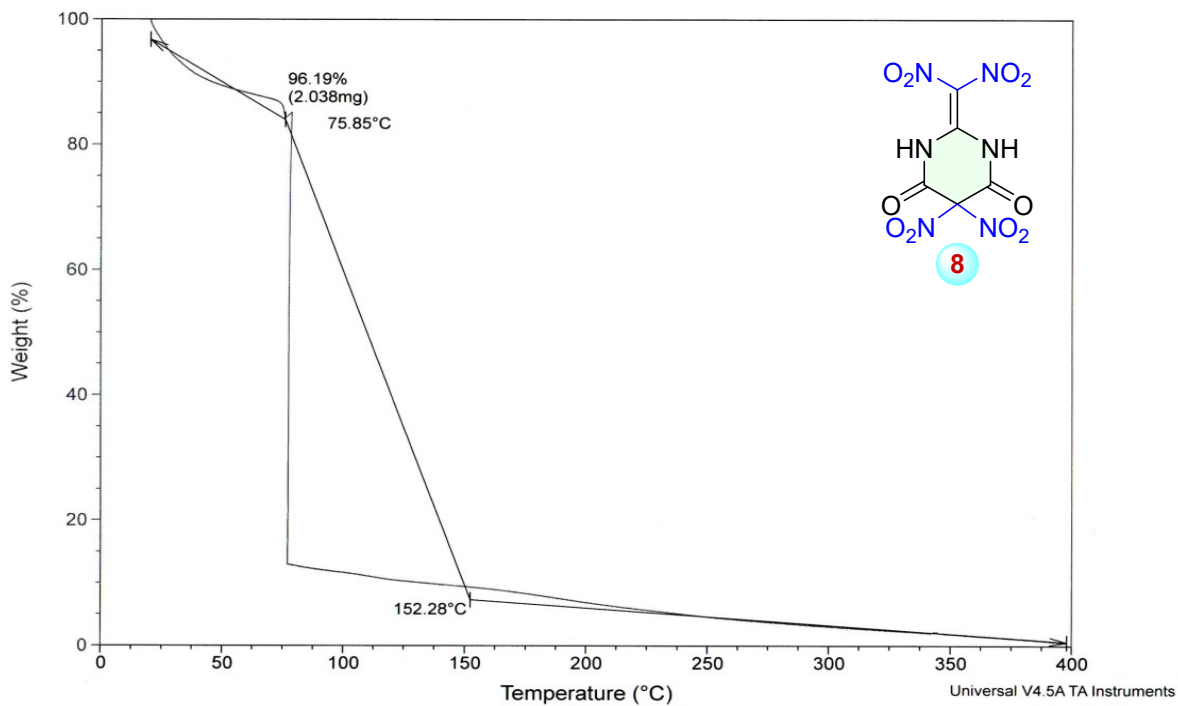


Fig. S37 TGA of compound 8 at 5 °C min⁻¹

Sample: SOHAN-619 at 5°C
Size: 1.8150 mg
Method: Ramp

TGA

File: C:\...TGA\SOHAN\SOHAN-619 at 5°C.001
Operator: SOHAN
Run Date: 10-May-2023 12:34
Instrument: TGA Q50 V20.13 Build 39

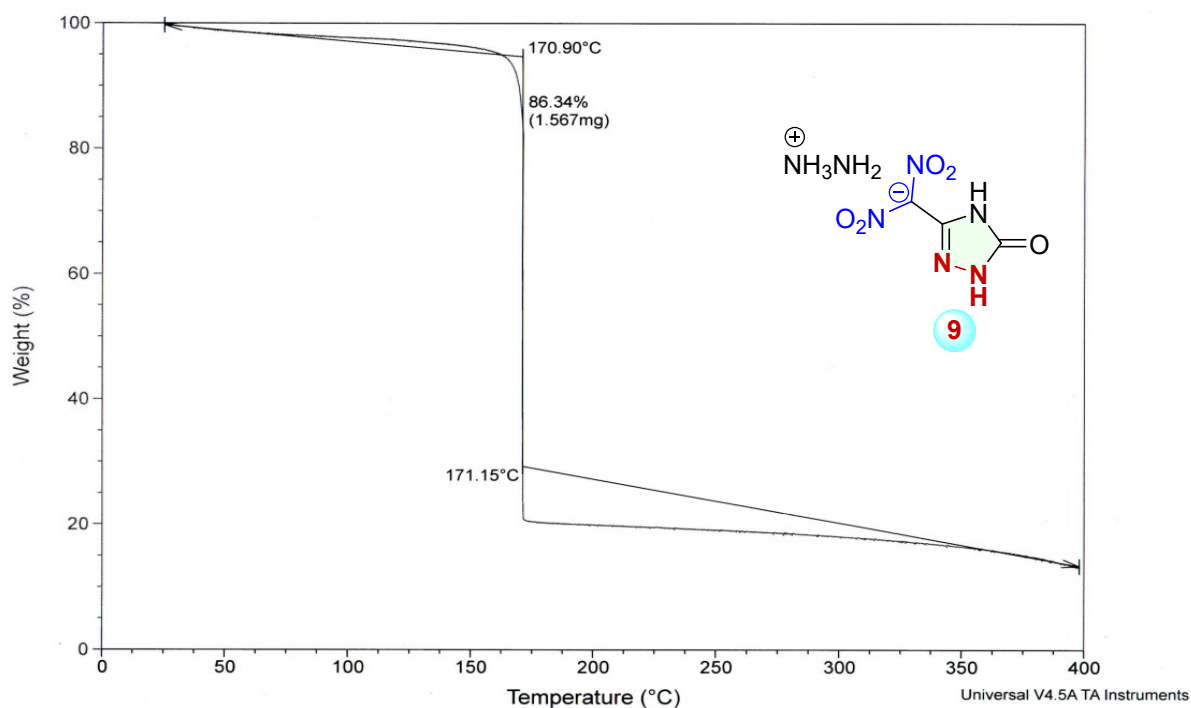


Fig. S38 TGA of compound 9 at 5 °C min⁻¹

Sample: SOHAN-619 at 10°C
Size: 2.2290 mg
Method: Ramp

TGA

File: C:\...TGA\SOHAN\SOHAN-619 at 10°C.001
Operator: SOHAN
Run Date: 10-May-2023 11:17
Instrument: TGA Q50 V20.13 Build 39

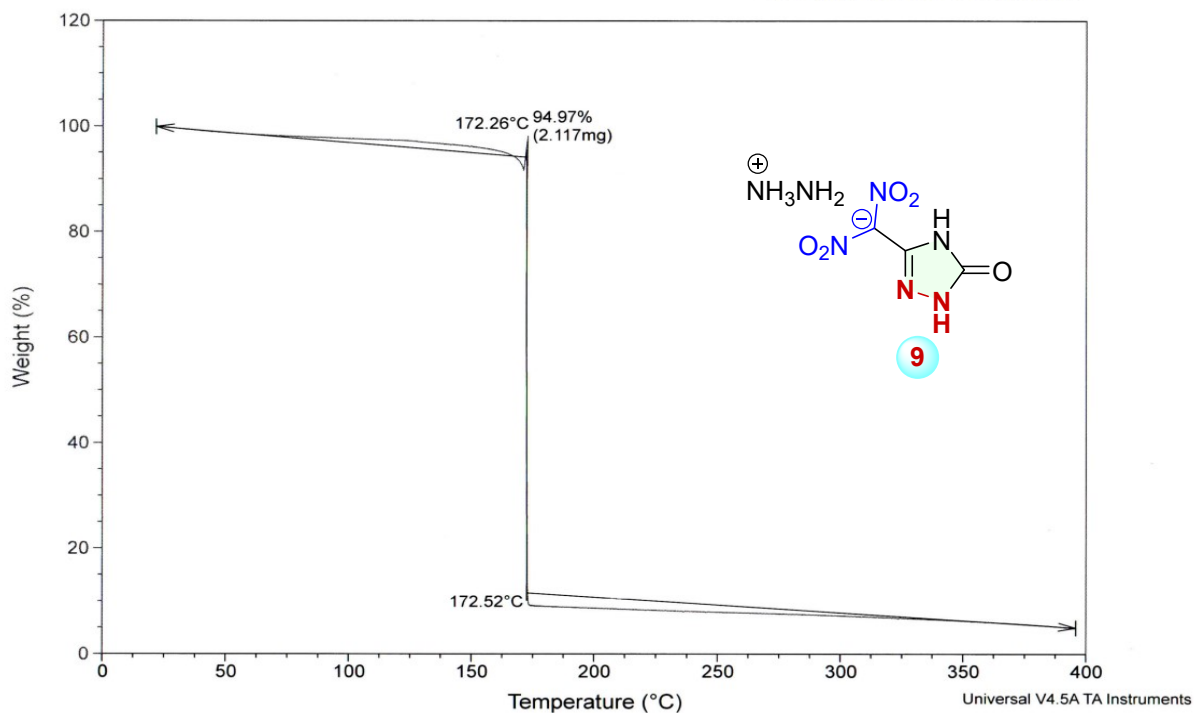


Fig. S39 TGA of compound 9 at 5 °C min⁻¹

Sample: SOHAN-623RR at 10°C
Size: 1.9220 mg
Method: Ramp

TGA

File: C:\...TGA\Sohan\SOHAN-623RR at 10°C.001
Operator: SOHAN
Run Date: 23-May-2023 20:35
Instrument: TGA Q50 V20.13 Build 39

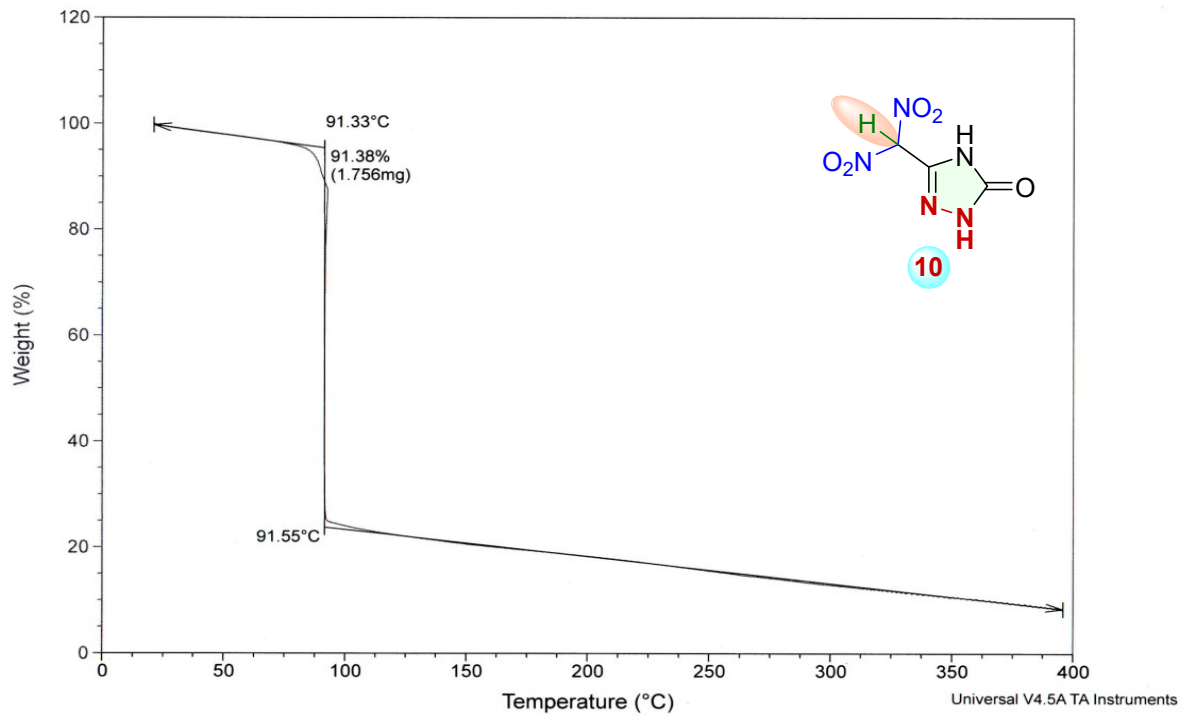


Fig. S40 TGA of compound 10 at 5 °C min⁻¹

Sample: SOHAN-626 at 5°C
Size: 2.0340 mg
Method: Ramp

TGA

File: C:\...TGA\Sohan\SOHAN-626 at 5°C.001
Operator: SOHAN
Run Date: 01-Jun-2023 16:56
Instrument: TGA Q50 V20.13 Build 39

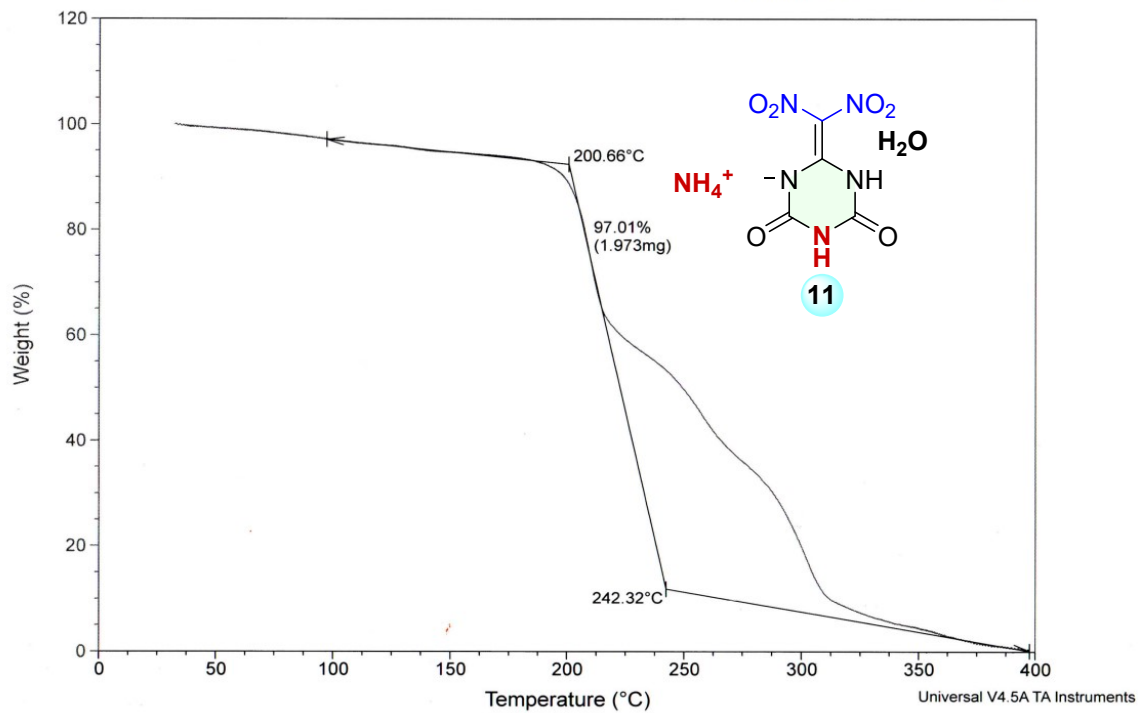


Fig. S41 TGA of compound 11.H₂O at 5 °C min⁻¹

Sample: SOHAN-FOX-7 at 5°C
 Size: 2.3290 mg
 Method: Ramp

TGA

File: C:\...TGA\Sohan\SOHAN-FOX-7 at 5°C.001
 Operator: SOHAN
 Run Date: 21-Dec-2022 13:42
 Instrument: TGA Q50 V20.13 Build 39

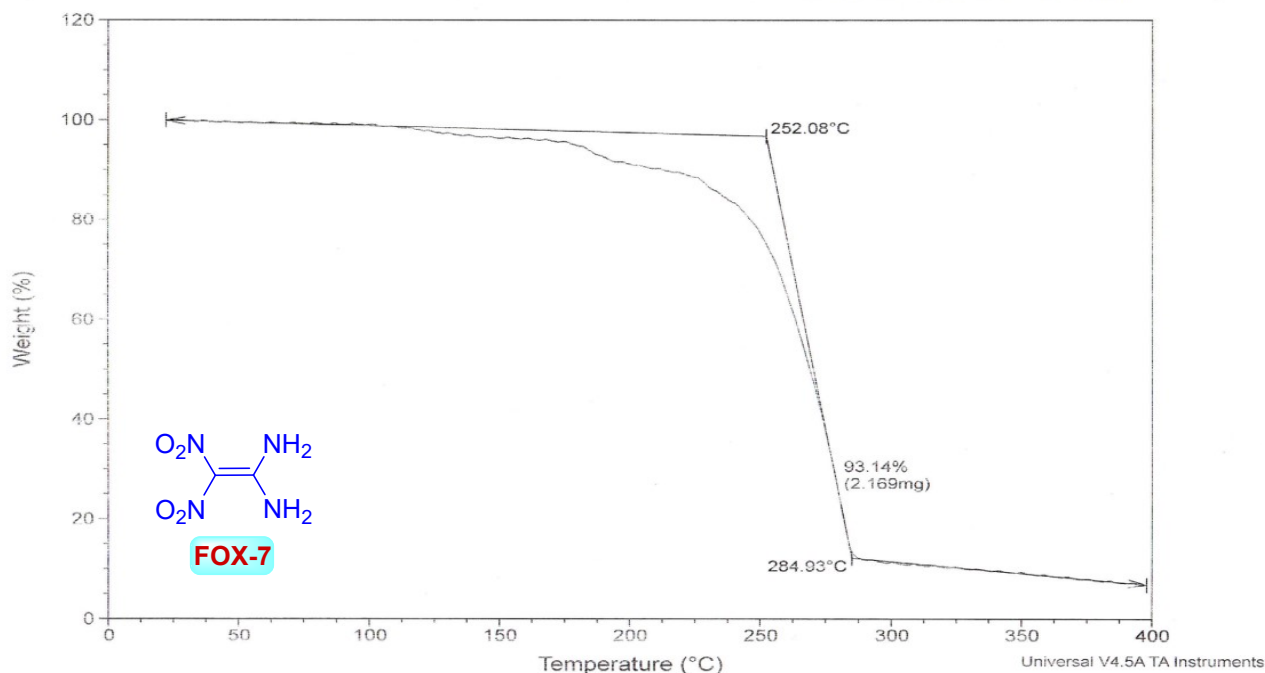
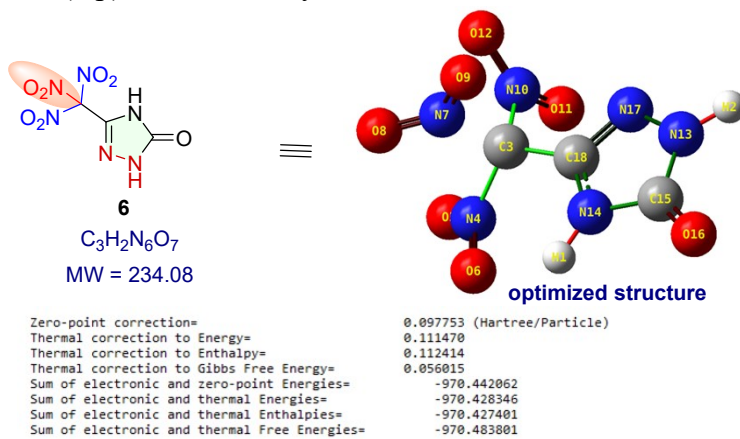


Fig. S42 TGA of compound FOX-7 at 5 °C min⁻¹

Table S13. Cartesian coordinates (in Å) for optimized structure of compound 6 obtained using the B3LYP/6-311++G(d,p) level of theory

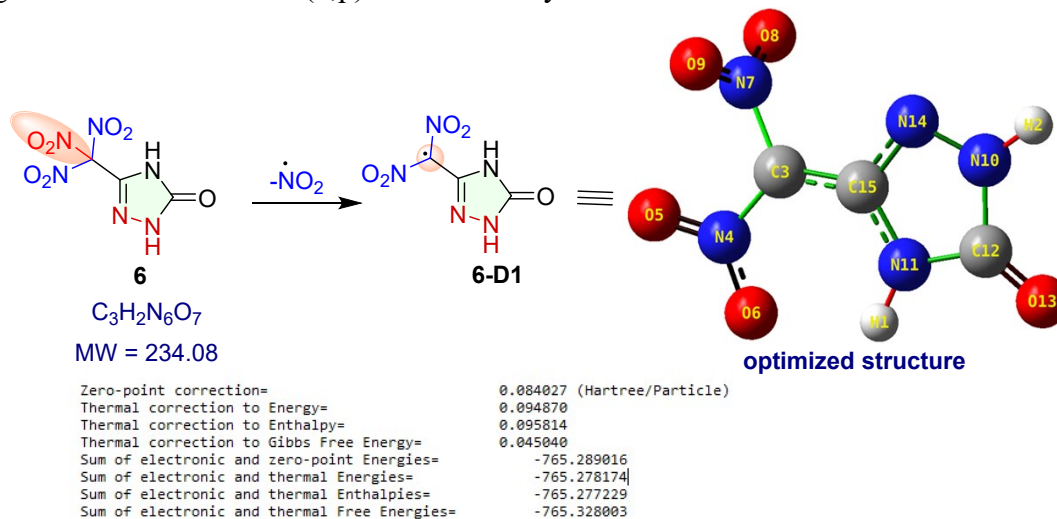


Center Number	Atomic Symbol	Coordinates (Angstroms)		
		X	Y	Z
1	H	-0.001367	4.334601	0.062278
2	H	0.829129	6.852583	-3.063359
3	C	-2.109598	6.299167	0.185123
4	N	-2.838334	5.009304	0.634443
5	O	-4.041143	5.014146	0.656434
6	O	-2.087475	4.105848	0.963063
7	N	-1.638105	6.980014	1.543516
8	O	-2.315724	6.747190	2.516325
9	O	-0.653865	7.671811	1.453880
10	N	-3.144603	7.253918	-0.464646
11	O	-3.657119	6.827539	-1.470876
12	O	-3.335113	8.310339	0.093174
13	N	0.429464	6.406913	-2.252024
14	N	0.001453	5.108857	-0.584404

15	C	0.956049	5.295414	-1.594947
16	O	1.953298	4.662553	-1.832741
17	N	-0.733435	6.858987	-1.731132
18	C	-0.978142	6.060208	-0.735905

Number of imaginary frequencies at the B3LYP/6-311++G(d,p) level = 0

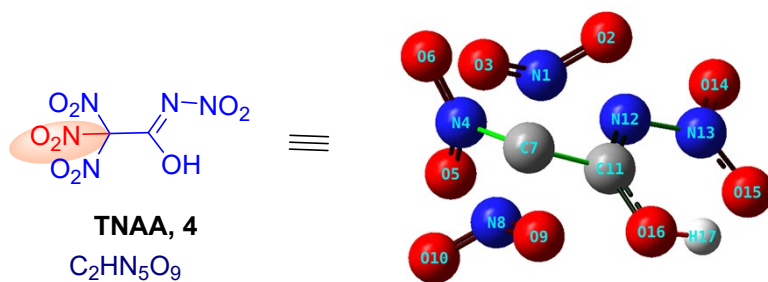
Table S14. Cartesian coordinates (in Å) for optimized structure of compound 6-D1 obtained using the B3LYP/6-311++G(d,p) level of theory



Center Number	Atomic Symbol	Coordinates (Angstroms)		
		X	Y	Z
1	H	-0.216997	4.298060	0.004686
2	H	1.050832	6.857733	-2.962600
3	C	-2.313046	6.137974	-0.288097
4	N	-2.799960	5.286427	0.737363
5	O	-3.922378	5.495801	1.176801
6	O	-2.043872	4.373875	1.108273
7	N	-3.205757	7.246398	-0.679880
8	O	-3.850401	7.091975	-1.700321
9	O	-3.211257	8.216340	0.054411
10	N	0.521191	6.389577	-2.240233
11	O	-0.131605	5.031188	-0.686721
12	C	0.952808	5.248959	-1.529088
13	O	1.987409	4.649920	-1.644678
14	N	-0.682696	6.837203	-1.892183
15	C	-1.088831	5.985806	-0.919997

Number of imaginary frequencies at the B3LYP/6-311++G(d,p) level = 0

Table S15. Cartesian coordinates (in Å) for optimized structure of compound TNAA, 4 obtained using the B3LYP/6-311++G(d,p) level of theory



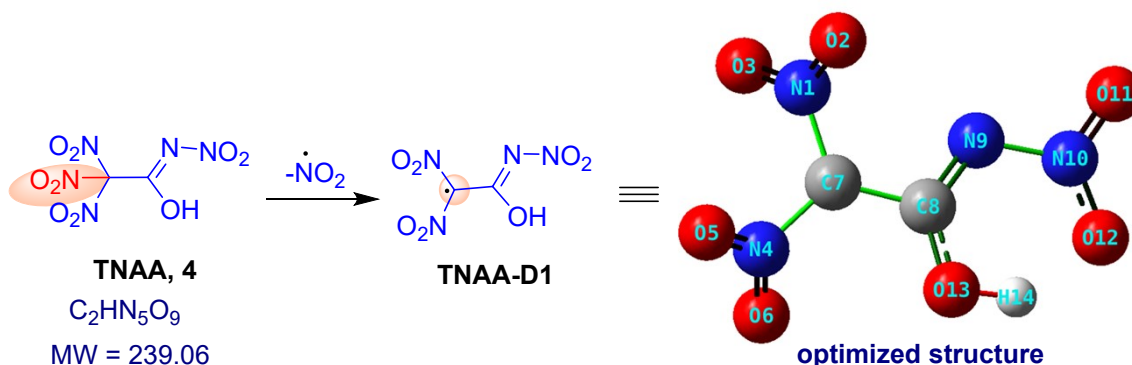
TNAA, 4
 $C_2HN_5O_9$
 MW = 239.06

Zero-point correction=	0.081330 (Hartree/Particle)
Thermal correction to Energy=	0.095638
Thermal correction to Enthalpy=	0.096582
Thermal correction to Gibbs Free Energy=	0.037574
Sum of electronic and zero-point Energies=	-1027.326554
Sum of electronic and thermal Energies=	-1027.312245
Sum of electronic and thermal Enthalpies=	-1027.311301
Sum of electronic and thermal Free Energies=	-1027.370309

Center Number	Atomic Symbol	Coordinates (Angstroms)		
		X	Y	Z
1	N	-4.318756	1.426156	0.462412
2	O	-4.132852	2.379699	1.183437
3	O	-5.347684	0.835749	0.241015
4	N	-3.200147	1.202725	-1.806394
5	O	-2.236794	0.871448	-2.457519
6	O	-4.215946	1.738721	-2.175780
7	C	-3.069615	0.877930	-0.293051
8	N	-3.128234	-0.669579	-0.081946
9	O	-3.271271	-0.991917	1.074768
10	O	-3.035113	-1.373130	-1.056051
11	C	-1.773451	1.487745	0.237378
12	N	-1.518739	2.657702	-0.246077
13	N	-0.349155	3.312636	0.233589
14	O	-0.160202	4.409794	-0.208011
15	O	0.393148	2.734608	1.053347
16	O	-1.129657	0.756464	1.099494
17	H	-0.325692	1.292069	1.360786

Number of imaginary frequencies at the B3LYP/6-311++G(d,p) level = 0

Table S16. Cartesian coordinates (in Å) for optimized structure of compound TNAA-D1 obtained using the B3LYP/6-311++G(d,p) level of theory



TNAA, 4
 $C_2HN_5O_9$
 MW = 239.06

Zero-point correction=	0.067022 (Hartree/Particle)
Thermal correction to Energy=	0.078763
Thermal correction to Enthalpy=	0.079707
Thermal correction to Gibbs Free Energy=	0.025540
Sum of electronic and zero-point Energies=	-822.157072
Sum of electronic and thermal Energies=	-822.145331
Sum of electronic and thermal Enthalpies=	-822.144386
Sum of electronic and thermal Free Energies=	-822.198553

Center Number	Atomic Symbol	X	Coordinates (Angstroms)		
			Y	Z	
1	N	-4.259286	1.666861	0.122107	
2	O	-4.323775	1.355089	1.294158	
3	O	-5.107927	2.223926	-0.549429	
4	N	-3.196461	0.415366	-1.701345	
5	O	-3.973092	-0.511820	-1.539226	
6	O	-2.557801	0.678113	-2.705358	
7	C	-3.025259	1.315285	-0.575705	
8	C	-1.738291	1.843872	-0.167633	
9	N	-1.816405	2.899505	0.603828	
10	N	-0.596721	3.454259	1.063327	
11	O	-0.707752	4.329928	1.877061	
12	O	0.489481	3.038621	0.609584	
13	O	-0.691824	1.197951	-0.616406	
14	H	0.102990	1.715301	-0.313394	

Number of imaginary frequencies at the B3LYP/6-311++G(d,p) level = 0

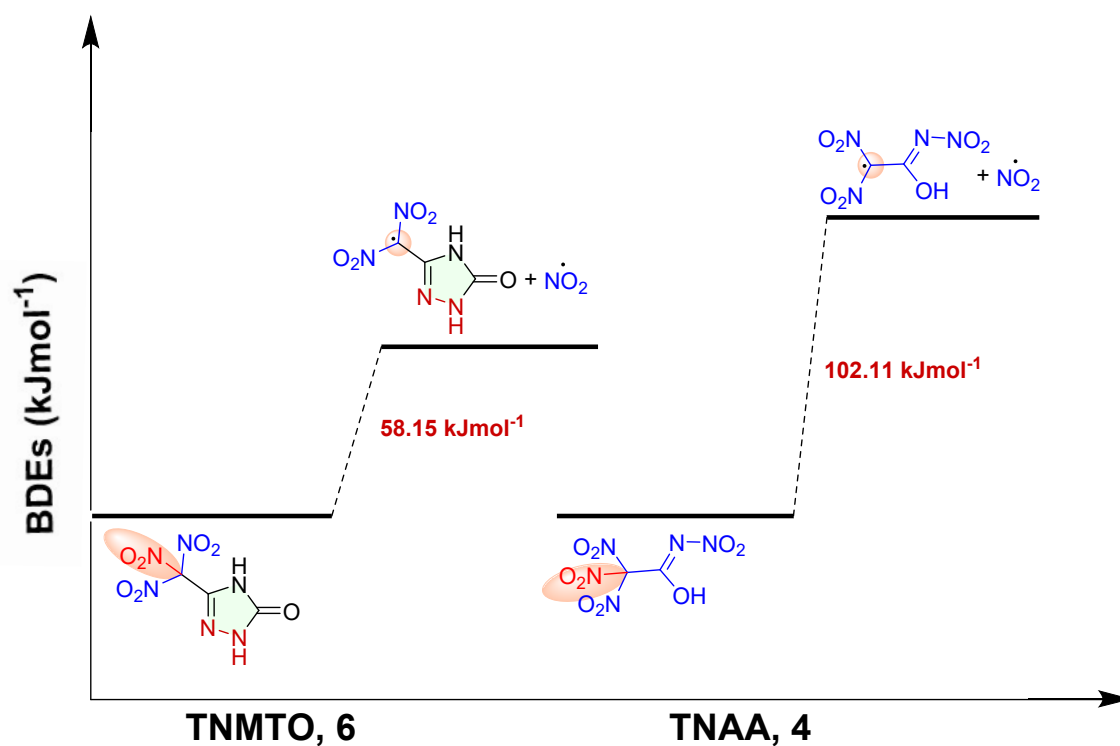


Fig. S43 Comparison of bond dissociation energies (BDEs), calculated at B3LYP/6-311++ G (d,p) level

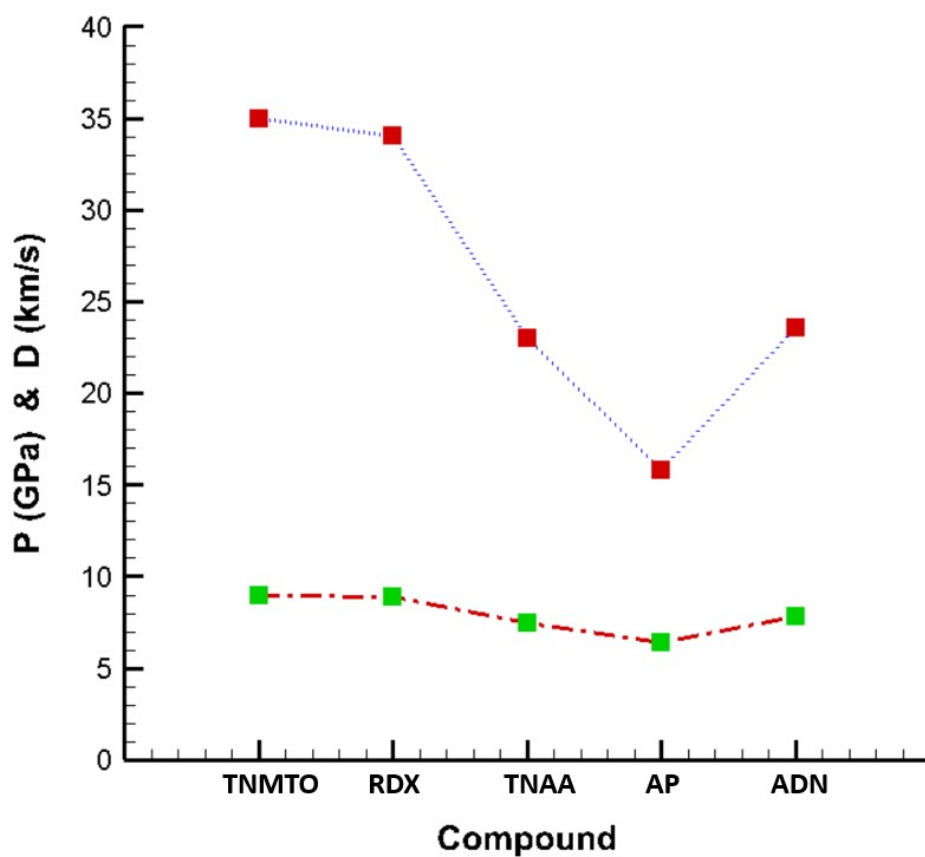


Fig. S44 Comparison of detonation velocity and detonation pressure.

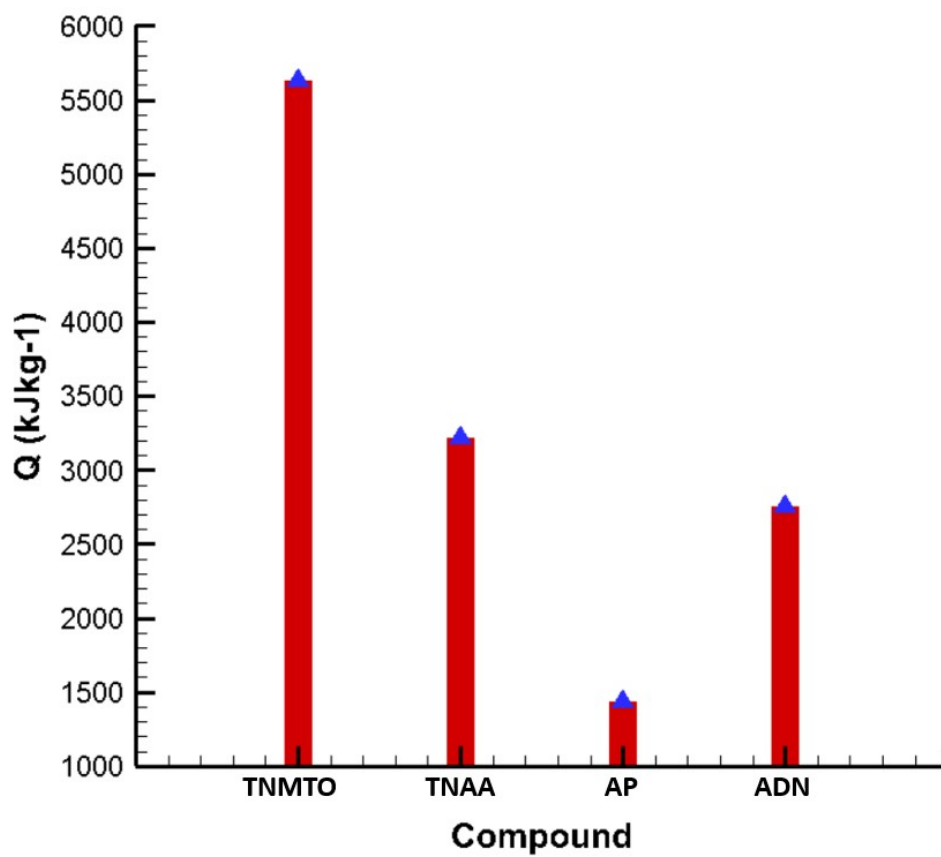


Fig. S45 Comparison of heat of detonation (Q).

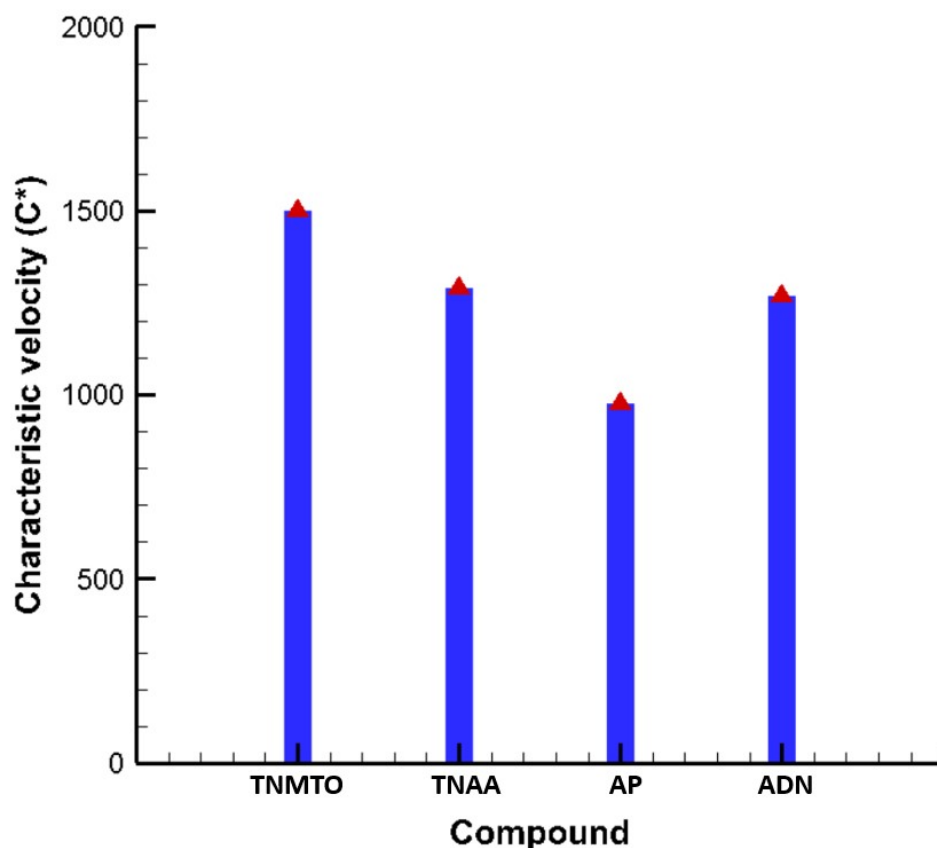


Fig. S46 Comparison of characteristic velocity (C^*).

REFERENCES

1. M. J. Frisch, G. W. Trucks, H. B. Schlegel, G. E. Scuseria, M. A. Robb, J. R. Cheeseman, G. Scalmani, V. Barone, B. Mennucci, G. A. Petersson, H. Nakatsuji, M. L. Caricato, X., H. P. Hratchian, A. F. Izmaylov, J. Bloino, G. Zheng, J. L. Sonnenberg, M. Hada, M. Ehara, K. Toyota, R. Fukuda, J. Hasegawa, M. Ishida, T. Nakajima, Y. Honda, O. Kitao, H. Nakai, T. Vreven, J. A. Montgomery, Jr., J. E. Peralta, F. Ogliaro, M. Bearpark, J. J. Heyd, E. Brothers, K. N. Kudin, V. N. Staroverov, R. Kobayashi, J. Normand, K. Raghavachari, A. Rendell, J. C. Burant, S. S. Iyengar, J. Tomasi, M. Cossi, N. Rega, N. J. Millam, M. Klene, J. E. Knox, J. B. Cross, V. Bakken, C. Adamo, J. Jaramillo, R. Gomperts, R. E. Stratmann, O. Yazyev, A. J. Austin, R. Cammi, C. Pomelli, J. W. Ochterski, R. L. Martin, K. Morokuma, V. G. Zakrzewski, G. A. Voth, P. Salvador, J. J. Dannenberg, S. Dapprich, A. D. Daniels, Ö. Farkas, J. B. Foresman, J. V. Ortiz, J. Cioslowski and D. J. Fox, Revision D.01 ed., Gaussian, Inc., Wallingford, CT, 2003.
2. P. W. Atkins, Physical Chemistry, Oxford University press: Oxford 1982.
3. M. S. Westwell, M. S. Searle, D. J. Wales and D. H. Williams, Empirical correlations between thermodynamic properties and intermolecular forces, *J. Am. Chem. Soc.*, 1995, 117, 5013–5015
4. H. Gao, C. Ye, C. M. Piekarski and J. M. Shreeve, Computational characterization of energetic salts, *J. Phys. Chem. C*, 2007, 111, 10718–10731.

5. M. S. Westwell, M. S. Searle, D. J. Wales, D. H. Williams, Empirical correlations between thermodynamic properties and intermolecular forces, *J. Am. Chem. Soc.*, 1995, 117, 5013-5015.
6. G. M. Sheldrick, Crystal structure refinement with SHELXL, *Acta Crystallogr. Sect. A Found. Adv.*, 2015, C71, 3-8.
7. G. M. Sheldrick, A short history of *ShelX*, *Acta Cryst.*, 2008, A64, 112-122.
8. Twin reference: S. Parsons, Introduction to twinning *Acta Cryst.*, 2003, D59, 1995-2003.
9. (a) CrysAlisPro Software System, Rigaku Oxford Diffraction, 2020. (b) G. M. Sheldrick, ShelXT-Integrated space-group and crystal-structure determination, *Acta Cryst.*, 2015, A71, 3-8.
10. O. V. Dolomanov, L. J. Bourhis, R. J. Gildea, J. A. K. Howard and H. Puschmann, OLEX2 A complete structure solution, refinement and analysis program. *J. Appl. Crystallogr.*, 2009, 42, 339-341.